

**REPUBLIC OF TURKEY
ISTANBUL GELISIM UNIVERSITY
INSTITUTE OF GRADUATE STUDIES**

Department of Electrical and Electronics Engineering

**MODELING AND ANALYSIS OF VOLTAGE SAG
MITIGATION TECHNIQUES IN LOW VOLTAGE
NETWORKS CONTAINING SOLAR PV UNITS**

Master Thesis

Riyam Muthanna Sabry AL-SAMMARRAIE

Supervisor

Asst. Prof. Dr. Yusuf Gürçan ŞAHİN

Istanbul – 2023

THESIS INTRODUCTION FORM

Name and Surname : Riyam Muthanna Sabry AL-SAMMARRAIE

Language of the Thesis : English

Name of the Thesis : Modeling and Analysis of Voltage Sag Mitigation Techniques in Low Voltage Networks Containing Solar PV Units

Institute : Istanbul Gelisim University Institute of Graduate Studies

Department : Electrical and Electronics Engineering

Thesis Type : Master

Date of the Thesis : 22.2.2023

Page Number : 103

Thesis Supervisors : Asst. Prof. Dr. Yusuf Gürcan ŞAHİN

Index Terms : Solar PV, Voltage Level Improvement, Voltage Stability, Harmonic Distortion.

Turkish Anstract : Bu araştırma, alçak gerilim dağıtım şebekelerindeki gerilim seviyesinin bozulması sorununu, Bağdat-Batı'daki 11 kV'luk bir trafo merkezindeki bir vaka çalışması aracılığıyla araştırmıştır. Çalışma, bir Solar PV dağıtılmış üretim (DG) ünitesi tasarlamak için yola çıktı ve tüketicilere arzın sürekliliğini iyileştirmenin yanı sıra dağıtım sistemlerindeki gerilim sarkma sorunlarına olası bir çözüm olarak önerdi. Bu güneş enerjisi üniteleri, başlangıçtaki DC jeneratörleri gibi, bu nedenle tipik olarak DC'den AC'ye dönüştürücüler olarak işlev gören PV invertörleri aracılığıyla şebekeyle arabirim oluşturur. Bu

nedenle, güneş PV üniteleri, şebeke voltajı performans seviyesini artıracak ayarlanabilir aktif güç (P) ve reaktif güç (Q) güç enjeksiyonlarına sahip güç kaynakları olarak kabul edilir. Bu öneriyi doğrulamak için, dağıtım trafo merkezinin simülasyonu, modern Elektriksel Geçici Analiz Programı (ETAP) kullanılarak gerçekleştirilir. Trafo merkezi veri sayfaları programa giriş verisi olarak beslenir ve simülasyon çalışmalarının sonuçları yük akış analizi, statik VAR kompanzasyonu ve harmonik bozulma analizi olmak üzere üç açıdan önemlidir.

Distribution List

- : 1. To the Institute of Graduate Studies of Istanbul
Gelisim University
2. To the National Thesis Center of YÖK (Higher
Education Council)

Riyam M. S. AL-SAMMARRAIE

**REPUBLIC OF TURKEY
ISTANBUL GELISIM UNIVERSITY
INSTITUTE OF GRADUATE STUDIES**

Department of Electrical and Electronics Engineering

**MODELING AND ANALYSIS OF VOLTAGE SAG
MITIGATION TECHNIQUES IN LOW VOLTAGE
NETWORKS CONTAINING SOLAR PV UNITS**

Master Thesis

Riyam Muthanna Sabry AL-SAMMARRAIE

Supervisor

Asst. Prof. Dr. Yusuf Gürçan ŞAHİN

Istanbul – 2023

DECLARATION

I hereby declare that in the preparation of this thesis, scientific and ethical rules have been followed, the works of other persons have been referenced in accordance with the scientific norms if used, and there is no falsification in the user data, any part of the thesis has not been submitted to this university or any other university as another thesis.

Riyam M. S. AL-SAMMARRAIE

.../.../2023

TO ISTANBUL GELISIM UNIVERSITY
THE DIRECTORATE OF INSTITUTE OF GRADUATE STUDIES

The thesis study of Riyam Muthanna Sabry AL-SAMMARRAIE entitled “Modeling and Analysis of Voltage Sag Mitigation Techniques in Low Voltage Networks Containing Solar PV Units”, has been accepted as MASTER THESIS in the department of Electrical and Electronic Engineering by out jury.

Director
Asst. Prof. Dr. Sevcen KAHRAMAN

Member
Asst. Prof. Dr. Yusuf Gürcan ŞAHİN
(Supervisor)

Member
Asst. Prof. Dr. Kenan BUYUKATAK

APPROVAL

I approve that the signatures above signatures belong to the aforementioned faculty members.

... / / 2023

Prof. Dr. Izzet GUMUS
Director of the Institute

SUMMARY

Although economically justified, the penetration of solar generation units into the main grid is accompanied by power quality (PQ) problems. Such issues, as voltage deviations and harmonic distortions in bus voltage and load current waveforms, are major concerns today. The voltage level at load buses in low voltage (LV) distribution substations should be maintained to meet the specifications listed in PQ standards and satisfy its requirements. In this research, the voltage level at load buses of a distribution substation is studied through both load flow analysis by Newton-Raphson method and through harmonic distortion analysis. For this purpose, a real 11 kV substation was taken as a case study to visualize the effect of solar PV penetration into the substation. This is achieved by modeling the substation single line diagram embedded with 2 MW solar units using ETAP environment. The design steps for the solar PV system are performed at the first step. Then calculations by ETAP computer program are used to evaluate the voltage levels at load buses and specify the deviations in these voltage results as compared to the international regulations and standards (IEEE 519 and IEC 61000-3-4). Finally, the improvements on voltage level values offered by solar PV units as well as by static VAR compensators are discussed and the conclusions and recommendations are given.

Keywords: Solar PV, Voltage Level Improvement, Voltage Stability, Harmonic Distortion.

ÖZET

Ekonomik olarak gerekçelendirilse de güneş enerjisi üretim ünitelerinin ana şebekeye girmesine güç kalitesi (PQ) sorunları eşlik ediyor. Bara gerilimi ve yük akımı dalga biçimlerindeki gerilim sapmaları ve harmonik bozulmalar gibi sorunlar günümüzün en önemli sorunlarından. Alçak gerilim (AG) dağıtım trafo merkezlerindeki yük baralarındaki gerilim seviyesi, PQ standartlarında listelenen özellikleri ve gereksinimlerini karşılayacak şekilde korunmalıdır. Bu çalışmada, bir dağıtım trafo merkezinin yük baralarındaki gerilim seviyesi hem Newton-Raphson yöntemi ile yük akış analizi hem de harmonik bozulma analizi ile incelenmiştir. Bu amaçla, trafo merkezine solar PV penetrasyonunun etkisini görselleştirmek için gerçek bir 11 kV trafo merkezi örnek olay incelemesi olarak alınmıştır. Bu, ETAP ortamı kullanılarak 2 MW güneş enerjisi üniteleriyle gömülü trafo merkezi tek hat şemasının modellenmesiyle elde edilir. Güneş PV sistemi için tasarım adımları ilk adımda gerçekleştirilir. Daha sonra ETAP bilgisayar programı ile yapılan hesaplamalar ile yük baralarındaki gerilim seviyeleri değerlendirilmekte ve bu gerilim sonuçlarındaki uluslararası yönetmelik ve standartlara (IEEE 519 ve IEC 61000-3-4) göre sapmalar belirlenmektedir. Son olarak, güneş PV ünitelerinin yanı sıra statik VAR kompensatörleri tarafından sunulan voltaj seviyesi değerlerindeki iyileştirmeler tartışılmakta ve sonuçlar ve öneriler verilmektedir.

Anahtar Kelimeler: Solar PV, Gerilim Seviyesi İyileştirmesi, Gerilim Kararlılığı, Harmonik Bozulma.

TABLE OF CONTENTS

SUMMARY	i
ÖZET	ii
TABLE OF CONTENTS	iii
ABBREVIATIONS	vi
LIST OF TABLES.....	viii
LIST OF FIGURES	ix
PREFACE	xi

CHAPTER ONE

INTRODUCTION

1.1. Background	1
1.2. MG Overview.....	3
1.3. Photovoltaics (PV)	6
1.4. Harmonics in Power System	7
1.5. Power Quality Problems	10
1.6. Research Objectives	12
1.7. Thesis Structure and Organization	13

CHAPTER TWO

OVERVIEW OF VOLTAGE STABILITY IN LV NETWORKS

2.1. Voltage Stability	14
2.2. Mitigation by Custom Power Devices (CPD) Techniques	15
2.2.1. Using one CPD	16
2.2.2. Using multiple CPDs	24
2.3. Mitigation by Strategical Planned Techniques	27

CHAPTER THREE

ANALYSIS OF DISTRIBUTION SYSTEM WITHH SOLAR PV

3.1. Solar PV Basics.....	29
3.1.1. Solar Cell Principles:	29
3.1.2. Solar Cell's Electrical Equivalent Circuit:	29
3.1.3. Selection of Solar Module:	31
3.2. PV System Layout	32
3.2.1. PV Inverters' Topologies:	33
3.2.2. System Design:	35
3.2.3. PV Array Configuration:	36
3.3. Performance Analysis with solar PV	38
3.4. Modeling and Analysis using Software 'ETAP'	39

CHAPTER FOUR

ANALYSIS AND CALCULATIONS

4.1. Solar PV System Design	40
4.1.1. Design Calculations by "PVSYST" Software	40
4.1.2 Calculations of PV System Using Design Equations	42
4.1.3 Comparison Between the Two Methods	45
4.2. Baghdad West Distribution Network	33
4.2.1. Baghdad 400/132/33 kV Network	46
4.2.2 Baghdad West 33/11 kV Substation	47
4.2.3 ETAP Simulation of 33/11 kV Substation	48
4.3. Power Flow Case Studies	49
4.3.1. Case 1: without PV, without SVC	50
4.3.2 Case 2: without PV, with SVC	52
4.3.3 Case 3: with PV, with SVC	53
4.3.4 Case 4: Improvement of Bus Voltages	55
4.4. Harmonic Analysis	59
4.4.1. Harmonic Causes and Effects	59
4.4.2 International Standards on Harmonics	60
4.4.3 Harmonic Analysis by ETAP	61

4.4.4 Case Study: Harmonic Analysis using ETAP..... 62

CHAPTER FIVE

CONCLUSIONS AND RECOMMENDATIONS

5.1 Conclusions 71

5.2 Recommendations..... 73

REFERENCES..... 74

APPENDIX (A)..... 78

ABBREVIATIONS

<i>A</i>	:	Solar cell's curve fitting factor
<i>APF</i>	:	Active power filter
<i>CPD</i>	:	Custom Power Devices
<i>DES</i>	:	Distributed Energy Sources
<i>DG</i>	:	Distributed Generation
<i>DSTATCOM</i>	:	Distribution Static VAR Compensator
<i>DVR</i>	:	Dynamic Voltage Restorer
<i>ESS</i>	:	Energy Storage System
<i>FACTS</i>	:	Flexible AC Transmission System
<i>FFT</i>	:	Fast Fourier Transformation
<i>HF</i>	:	High Frequency
<i>I_(t)</i>	:	Current of cell, in Amp.
<i>I_{ph}</i>	:	Current generated by photovoltaic effect, in Amp.
<i>I_o</i>	:	Diode leakage current, in Amp.
<i>IEA</i>	:	International Energy Agency
<i>K</i>	:	Boltzmann constant (1.3805×10^{-23} J/K)
<i>LV</i>	:	Low Voltage
<i>MF</i>	:	Medium Frequency
<i>MG</i>	:	Microgrid
<i>MPPT</i>	:	Maximum Power Point Tracking
<i>PV</i>	:	Photovoltaic
<i>PQ</i>	:	Power Quality
<i>q</i>	:	Charge of electron (1.6×10^{-19} Coulomb)
<i>RES</i>	:	Renewable Energy Source
<i>R_s</i>	:	PV cell series resistance, in Ω
<i>R_{sh}</i>	:	PV cell shunt resistance, in Ω
<i>SAPF</i>	:	Shunt Active Power Filter
<i>SH</i>	:	Supraharmonic
<i>SSR</i>	:	Superconducting Shunt Resonator
<i>SVC</i>	:	Static VAR Compensator
<i>SVR</i>	:	Series Voltage Regulator

T	:	Cell temperature, in Kelvin
THD	:	Total Harmonic Distortion
T_m	:	Module temperature in °C.
T_{STC}	:	Temperature at standard test conditions (25 °C)
$ULTC$:	Under Load Tap Changer
$UPQC$:	Unified Power Quality Conditioner
V	:	Output voltage, in Volts
$V_{(t)}$:	Module voltage at any temperature
VSC	:	Voltage Source Converter
α_v	:	Temperature coefficient of V_{oc}
δ	:	The solar decline angle
ϕ	:	The location's latitude.
γ	:	The azimuth angle.

LIST OF TABLES

Table 1. PQ issues, causes and effects	10
Table 2. Literature review comparison for single CPD.....	22
Table 3. Literature review comparison for multiple CPDs	25
Table 4. Literature review comparison for strategical planned techniques.....	27
Table 5. Some brands of solar panel modules	31
Table 6. SUNPOWER brand electrical data	32
Table 7. PV project summery by PVSYST	33
Table 8. PV project layout by PVSYST	33
Table 9. PV system characteristics	40
Table 10. Brands and specifications of (> 500Wp) solar panels	42
Table 11. Solar inverter specifications	43
Table 12. Comparison between system layout from the two methods.....	28
Table 13. Study case 1, general results	50
Table 14. Study case 1, main grid results	50
Table 15. Study case 1, load flow results at busbars	50
Table 16. Solar inverter specifications	51
Table 17. Study case 2, SVC effects on grid performance.....	52
Table 18. Study case 3, general results	53
Table 19. Study case 3, main grid results.....	54
Table 20. Study case 3, load flow results at busbars	54
Table 21. Study case 3, load flow results at loads.....	55
Table 22. Study case 4, general results	55
Table 23. Study case 4, main grid results	56
Table 24. Study case 4, load flow results at busbars	56
Table 25. Study case 4, load flow results at loads	57
Table 26. Comparison between results of cases 3 and 4	58
Table 27. Harmonic voltages at system busbar vs. freq. spectrum (case A).....	65
Table 28. Harmonic voltages at busbar verified according to standard (case A).....	67
Table 29. System Harmonics Bus Information (case B)	69
Table 30. Harmonic Voltages as % of Fundamental Voltage (case B).....	69

LIST OF FIGURES

Figure 1. Historical, forecasted, and IEA Net Zero Scenario cumulative installed capacity and average annual renewable capacity additions, 2009–2026	1
Figure 2. Solar PV global installed capacity (GW) and its annual addition	3
Figure 3. Structure of a typical MG	4
Figure 4. Basic Photovoltaic Cell Circuit	6
Figure 5. Voltage waveform distortion due to current through the nonlinear load	8
Figure 1. Comparison between current waveforms and spectra. a) Pure sinusoidal. b) Distorted wave	8
Figure 7. Comparative overview of PQ issues contribution in power grids.	15
Figure 8. Distribution Static Synchronous Compensator (D-STATCOM).....	17
Figure 9. Block diagram of PV fed UPQC	18
Figure 10. Conceptual scheme of the proposed distribution transformer with power electronics module.	18
Figure 11. Schematic diagram of the DVR.....	19
Figure 12. The New DVR topology diagram	20
Figure 13. Shunt Active Power Filter (SAPF)	20
Figure 14. Principle of the proposed SSR	21
Figure 15. The LC resonant frequency circuit's natural decomposition properties. .	22
Figure 16. Equivalent circuit of the single-diode solar cell	21
Figure 17. Types of PV inverters (a) central, (b) string, (c) multi-string, and (d) module inverter.	34
Figure 18. Calculating the distance among Photovoltaic modules rows.....	37
Figure 19. Normalized productions (per installed kWp).....	41
Figure 20. The Performance Ratio PR	42
Figure 21. Two MW PV system layout	45
Figure 22. Baghdad city power grid	47
Figure 23. Baghdad city 33/11 kV distribution network.....	48
Figure 24. SLD of Baghdad West Substation Network (in ETAP Environment)	49
Figure 25. SVC rating effects on grid performance	53
Figure 26. Improvements offered by addition of PV units (case 4)	59
Figure 27. IEEE 519 (1992) vs IEEE 519 (2014)	60
Figure 28. THD viewed on the SLD of substation under study	63
Figure 29. Fundamental components viewed on the SLD of substation	63
Figure 30. 5 th harmonic components viewed on the SLD of substation	64
Figure 31. 7 th harmonic components viewed on the SLD of substation.....	64
Figure 32. 11 th harmonic components viewed on the SLD of substation	65
Figure 33. Percentage harmonic voltages at buses 1, 2, and 30 (case A).....	66
Figure 34. Percentage harmonic voltages at system load buses (case A).....	67

Figure 35. Percentage voltage THD at buses 1, 2, and 30 (Case B).....	68
Figure 36. Percentage voltage THD at load buses (Case B)	68
Figure 37. Harmonic Order Viewer on SLD of substation (Case B)	69
Figure A1. Example ANSI after running load flow analysis	78
Figure A2. Toolbar showing the Load Flow Analysis button location	79
Figure A3. Locations of essential buttons for the analysis	79
Figure A4. Helpful tips	80
Figure A5. Options viewed to display required results	81
Figure A6. Alert View button in the Load Flow toolbar	81
Figure A7. Setting the output report manager	82
Figure A8. Setting the Load Tap Changer for the transformer	83
Figure A9. Results could be shown on SLD view	84
Figure A10. Load Flow Result Analyzer	84

PREFACE

It is my pleasure here to express the due thanks to my professors, Yusuf Gürcan ŞAHİN and Saad T.Y. ALFALAHI, for their continual support during the entire time taken to accomplish this thesis. I would also like to express my appreciation and thanks to all the remarkable professors, and all the staff of Istanbul Gelişim University who accompanied us during our academic journey. I also wish to thank my family for their patience and support throughout my study period.

I would like to dedicate my thesis to my dear parents and my beloved children, wishing that one day they have the opportunity to read it and share with me their memories with joy and happiness.

CHAPTER ONE

INTRODUCTION

1.1. Background

The main reason for rising greenhouse gas emissions and high fossil fuel usage is the rapid development of world energy supply and consumption. The renewable energy generating industry has been prompted by pertinent worries to carry out a substantial study to ascertain ways to substitute conventional fossil fuels and lessen environmental issues. Accordingly, in recent years there has been a significant increase in Renewable Energy Sources (RESs) integration and installation into that is existed in power systems. As shown in Figure (1).

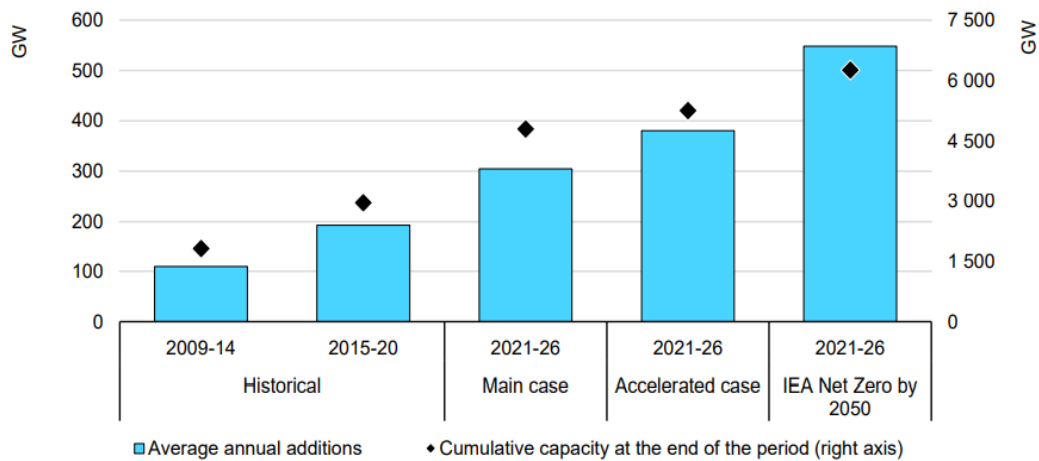


Figure 1. Historical, forecasted, and IEA net zero scenario cumulative installed capacity and average annual renewable capacity additions, 2009–2026 [1].

In late 2008, hydropower share of the total installed capacity of grid-connected RESs has fallen below 48per cent, accounting for no longer half of the total installed capacity. Solar PV currently provides for more than 20% of installed renewable power generating capacity, while wind power has increased to almost 25%. Currently, the amount of renewable in installed power generation capacity has increased to about 33%.

However, RESs have linked by means of the current district/decentralized energy (or as known as “Distributed generation” in addition to the Energy Storage System (ESS) because of their reliance on climatic factors, fuel types (such as fuel cells), and the energy storage systems (henceforth: ESSs) they produce. Additionally, several nations promote the linking of RES-based DGs to distribution networks (which is known as “distributed energy sources” (henceforth: DESs). So, the idea of a Microgrid (MG) is created and described as a collection of DESs and linked load operating as a single grid within explicitly defined electric limits.

The commercial adoption of solar PV technology means that it now only needs a small amount of labor to run, making solar farms simple to construct and quick to realize. Using data from historical meteorological stations or taking meteorological measurements is the only requirement, but it still has some problems that make these technologies insufficiently competitive with markets for fossil fuels. These problems include low solar cell conversion efficiency, high capital costs, extensive field daily maintenance and cleaning costs in dusty areas, and output power. Because of this, maximum power point tracking circuitry is required to exploit the PV system to its optimal capacity.

Cables and junction boxes, PV modules, grid-connected inverters, foundations and mounting structures, monitoring systems, medium-voltage equipment, and transformers (if necessary) are the essential parts of a PV system that is linked to the grid. Recent estimates show that solar energy has overtaken other renewable energy sources, with the installed capacity of all PV systems worldwide reaching (470 GW) in 2021, a figure around ten times more than 2011. Overall, the development of solar PV-producing units is rising, as shown in Figure (2), which depicts the yearly growth in solar energy use.

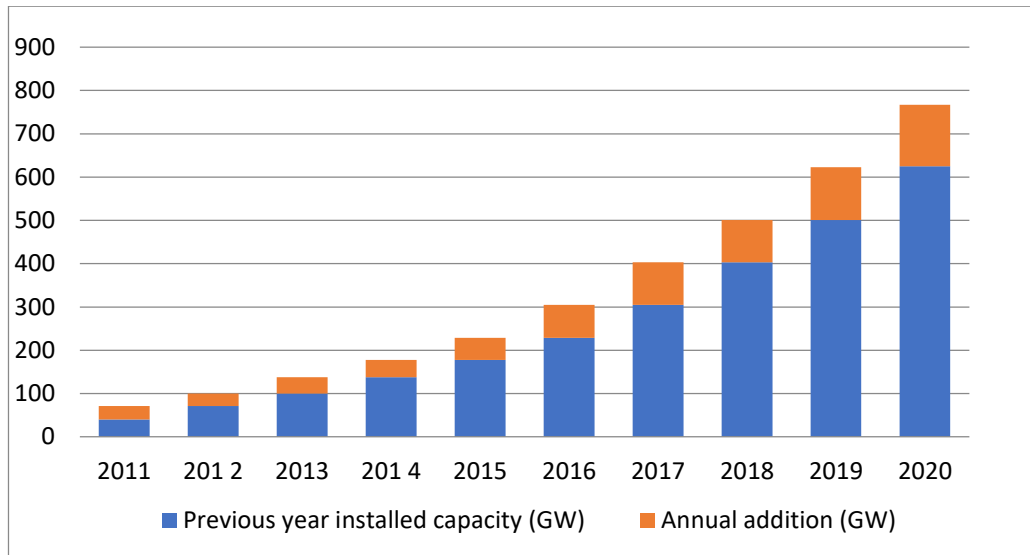


Figure 2. Solar PV global installed capacity (GW) and its annual addition

1.2. MG Overview

The Microgrid (MG) is important in developing a smart grid. It is a small-scale power system using dispersed energy resources. Adopting a system in which the related loads and generation are treated as a subsystem, or a MG is crucial for realizing the promise of distributed generation. First, the types and design of MGs are discussed, and then the purpose of MG control is described. MGs are regarded as feasible alternatives for locations where main grid extension is either impractical or unjustifiable financially, like the electrification of universities, military sites, and rural communities. It is possible to think about MG as a particular type of distribution system with distributed generators that can run in either an islanded (stand-alone) mode or grid connected. Even while the distribution system and the MG contain some features, such as customer kinds and voltage level, the MG has unique structures all its own. So, Figure (3) shows that MG consists of (DC to DC and/or DC to AC converters, Unstable loads demand on multiphase lines and each phase, Energy storage, Backup generators and Renewable sources).

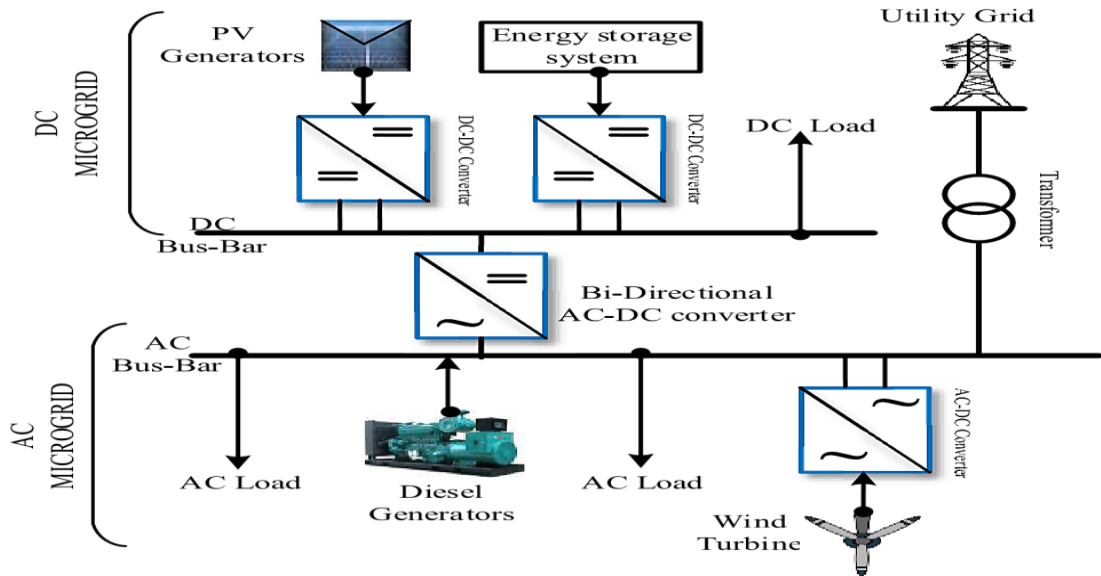


Figure 3. Structure of a typical MG [2].

This unique construction enables both stand-alone and grid-connected modes, two of MG's key advantages, to supply electricity whether or not there is a grid-side power outage. Along with this advantageous benefit, maintaining the system's security and efficiency might provide difficulties. The issue of electrical power quality is one of the primary issues in the MG study. For the benefit of consumers and equipment, it is crucial to evaluate electrical power quality based on extensive expertise.

The idea of MG is brand new and only emerged in the last ten years. There is no clear description of MG; however, researchers do agree on several of its features. It operates at a low voltage level, typically at the same voltage as the distribution system. The MG idea considers a group of loads and micro-sources as a single, controlled system that supplies electricity to its immediate surroundings [3]. MGs are typically viewed as feasible alternatives for locations where main grid extensions are either impractical or lack sufficient economic reason, such as the electrification of universities, military sites, and rural communities [3].

In conventional power systems, one source supplies the whole system due to its one-way construction architecture. Consequently, in a normal power system, electricity may flow in only one direction. However, these micro-sources may be put everywhere with MG and are also known as distributed generators (DGs). DGs come in various forms, including energy storage, solar, wind, and tiny gas turbines. The primary goal of MG is to provide local services before achieving autonomous

operation with less emissions. Large-capacity energy sources are impractical for this use; small-scale renewable energy might be crucial.

According to some researchers, the MG is a particular type of distribution system that includes DGs and may function either as islanded (stand-alone) or linked to the grids [2]. Due to the relatively tiny size of micro-sources, the main grid controls most of the system-level dynamics in grid-linked modes; in the micro-sources themselves, their power regulation control, stand-alone mode, and an uncommon extent, the network itself, govern the system dynamics [3]. Additionally, even when MG is operating in grid-connected mode, the connection with the grid should be turned off if a fault occurs in the MG to safeguard the grid. Therefore, the ability of DGs and energy storage to completely supply the load demand is not always assured. In this situation, certain loads must have their power supply switched off; these loads are non-critical loads, whilst other loads must have their power supply maintained for 24 hours, which are critical loads, as shown in Figure (3), which depicts a typical MG.

Due to this unique structure, which also has this advantageous feature, there may be difficulties maintaining the system's security and reliability. The issue of electrical power quality is one of the primary issues in the MG study.

Scholars create and test filters to address harmonic distortion. Passive power filters are less expensive and have fewer parts than active power filters. Meanwhile, fixed passive filters may support reducing harmonic on the default order settings; their effectiveness can be severely restricted when harmonic distortions are severe and fewer expected. Unfortunately, most studies that looked at inverter controls or filter designs are primarily interested in power electronics, independent of the harmonic's response in the MG. For harmonics problems, active power filters have been studied.

Power quality harmonics distortion is influenced by a wide range of parameters. Therefore, for better simulation outcomes, energy storage, weather, inverters, DGs, and load modelling must all be combined in the harmonic's studies. The next chapters offer a detailed analysis.

1.3. Photovoltaics (PV)

In Photovoltaic (PV), semiconductors are lit by photons to produce Direct Current (DC) Electrical Power that is measured in watts (W) or kilowatts (kW). Figure (4) illustrates a basic approach for the mathematical analysis of the PV module and simulation work.

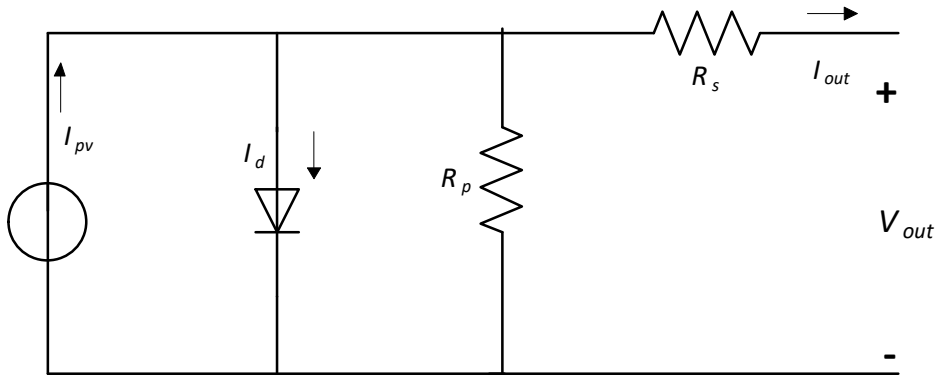


Figure 4. The Basic Photovoltaic Cell Circuit

Many academics believe that PV is the answer to the energy problem since the power of solar irradiation over the entire planet may be deemed endless for humans. Solar cells, which are made up of PV cells, are frequently seen on residential rooftops nowadays. On a few specific household appliances, like heating water, they function effectively. Utility-scale solar farms are being researched and constructed more often with the goal of letting solar energy replace more conventional electricity. In addition, to Photovoltaic panels are utilized to control direct current voltage after photovoltaic output. Maximum Power Point Tracking (MPPT) and converters are used for PV sources. Researchers have created numerous control schemes for MPPT due to the characteristics of PV cells, allowing them to produce the greatest power possible under certain weather conditions. Inverters must be installed after converters if a PV source is linked to an AC system. Utility-scale solar farms typically have a capacity of more than 500 kW. “The total global grid-connected solar PV capacity rose in just seven years, from 2004 to 2010, at an average annual rate of 55 per cent, reaching a capacity of around 40 GW” [4]. Even though this new application has a lot of potential benefits, there are still some technical issues.

Three main categories of the previous study on solar PV applications in power systems can be made: modelling, technological effect, and financial planning [4]. Harmonics analysis is one of the most crucial aspects of power quality research. Inverters are regarded as generators of current harmonics in PV sources.

Large-scale PV sources require vast spaces. PV sources will have significantly more options to serve MG rather than directly connecting to the transmission grid because to the size restriction on PV farms and the ideal location for solar irradiation.

1.4. Harmonics in Power System

The use of renewable energy has changed the way that electrical sources produce power. Renewable Energy Systems (RES) and nonlinear loads are the two primary harmonic contributors in power systems [5]. It's essential to describe harmonics occurrences in order to comprehend their impacts. In this regard, for linear loads, the load current is typically influenced by the load current quality, which in turn is influenced by the grid voltage quality. Figures (5) and (6) show that the voltage waveform distortion causes a distortion in the current waveform before further distorting the voltage waveform [5]. Even when the supply voltage is almost entirely sinusoidal, the distortion effect tends to be greater and more complex because the load pulls a distorted current. As a result, the circuit converts a sinusoidal supply voltage into a non-sinusoidal load voltage.

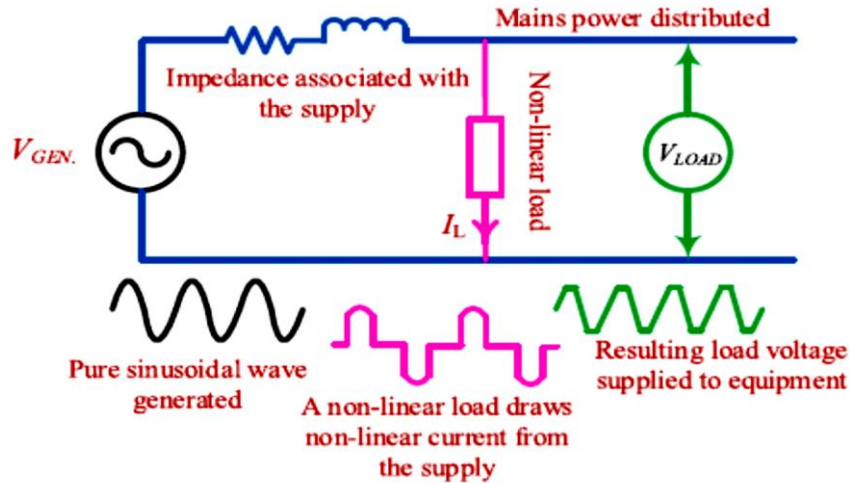


Figure 5. Voltage waveform distortion due to current through the nonlinear load [5].

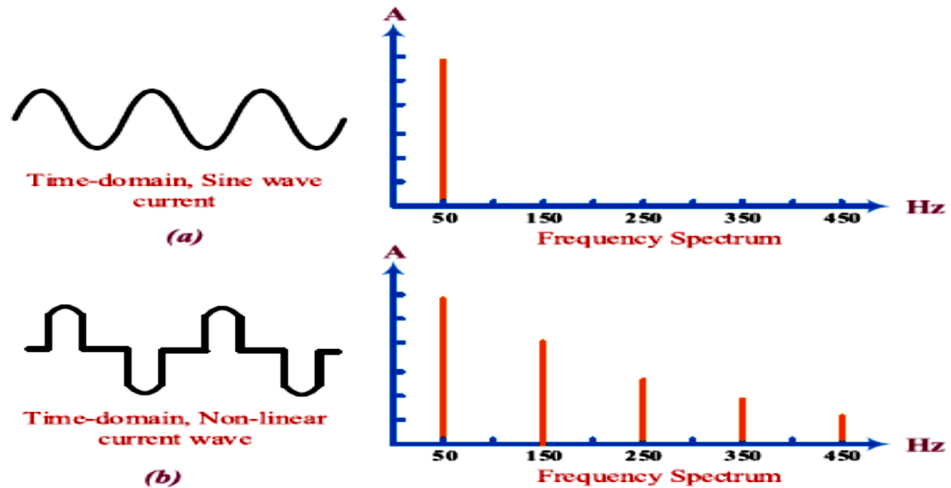


Figure 6. Comparison between current waveforms and spectra. a) Pure sinusoidal. b) Distorted wave [5].

Studying the full model of each component might help with the goal of understanding what the output of renewable energy sources might be. In particular, PV sources should be investigated since it is frequently integrated into local low voltage level MG. Given the tiny size of the loads and generation in MG, the harmonics created by PV will have a greater impact than in a traditional big grid, leading to issues including overheated electronics, poor power quality, and power loss. Certainly, utility companies are interested in finding a remedy to lessen those adverse effects as well as customers. But first, researchers need to figure out how to

characterize, analyze, and measure harmonics in MG before they can truly come up with a solution for this issue.

The ideal frequency for the world's electricity systems is 50 Hz. Harmonic components do, however, continuously exist in currents and voltages for a variety of reasons. Data from measurements demonstrate that the current or voltage waveforms are a superposition of the fundamental frequency and several harmonic components in the temporal domain. The signals can be examined in the frequency field in order to apply Fast Fourier Transformation (FFT).

Total Harmonic Distortion (THD) is taken into account to measure the harmonic of electrical parameters, counting currents and voltages. In the analysis of power systems, keeping an eye on THD value is crucial. Most electrical equipment and components in the grid are built to operate with voltages and sinusoidal-wave currents at a specific frequency. Different higher-order frequencies of current and voltage can damage components and reduce their lifespan. Another effect of harmonics is that they can cause components to overheat, like transformers, which increases losses. Due to these detrimental effects of harmonics in the power system, researchers have analyzed and developed harmonic solutions.

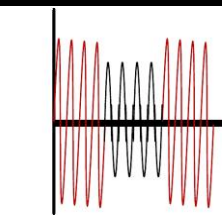
Harmonic research demands a distinct modelling approach from static power flow analysis that can precisely characterize the behavior of components at various frequencies. Transmission lines may also experience resonance phenomena because capacitors and inductors react differently under higher frequency conditions. The resonance occurs when the reactance of the inductor and capacitor cancels. The current near resonant frequency dominates significantly more than other frequencies in the FFT harmonic spectrum.

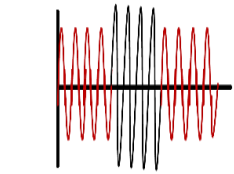
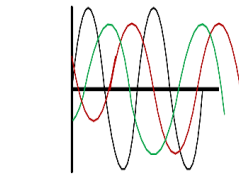
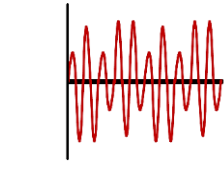
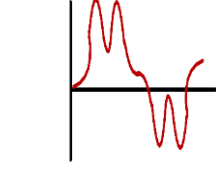
Active power filters (APF), one of the numerous efficient methods for mitigating harmonics in the power system, have drawn much attention from academics.

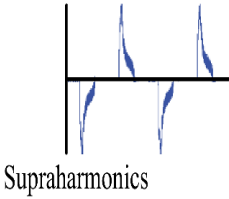
1.5. Power Quality Problems

The widespread use of MG significantly reduces CO₂ emissions and aids in reducing the effects of climate change. However, power quality (PQ) problems are one of the most pertinent technical difficulties with the operation and control of grid-connected MG or independent systems. Due to the MG system's structure, operating mode, and performance, these issues are of great significance [2]. The most significant PQ issues brought on by the high DG penetration are illustrated in Table 1-1 [2]. The European power quality study indicated that the sector would suffer a significant economic loss as a result of power quality concerns in the European Union. The industry sector in the poll was responsible for 90 per cent of this loss. Data from 62 businesses in various industries and service areas were gathered for the study [6]. The assessment lists the industry's production losses, equipment losses, work expenses, and labor costs. PQ problems cause both financial costs from replacing system components and output losses in the business sectors. Therefore, increasing PQ is crucial economically. Maintaining power distribution bus voltages and currents at their rated magnitude and frequency is referred to as PQ [2]. Since the voltage produced by sources like wind, solar, and fuel cells is very erratic, these sources cannot be directly linked to the grid. The PQ issues that were introduced in various DG units are presented in Table (1) [2].

Table 1. PQ issues, causes and effects [2]

PQ problem	Brief Description	Causes	Effects
	<p>The voltage levels decrease at the nominal frequency by 10% to 90% of the nominal RMS voltage over a period ranging from 0.5 cycles to 1 min.</p>	<ul style="list-style-type: none"> -Abrupt load rises -Faults -Motors starting -Energization of heavy loads 	<ul style="list-style-type: none"> -Can damage the MGs power electronics devices -High power loss -Damage sensitive load equipment -Speed loss for motors -Extinguishing of lighting lamps

PQ problem	Brief Description	Causes	Effects
 <p>Swell</p>	<p>The voltage levels increase at the nominal power frequency over the period not exceeding 1 cycle and less than 1 min</p>	<ul style="list-style-type: none"> -Abrupt load reduction -De-energization of heavy loads 	<ul style="list-style-type: none"> -Breakdown of components of the power supplies of the equipment -Control problems and hardware failure -Overheating
 <p>Unbalance</p>	<p>A variation of voltage in the three-phase system where the difference between phase angle and magnitude is not equal</p>	<ul style="list-style-type: none"> -Variations in the load -Large single-phase loads -Unequal load distribution 	<ul style="list-style-type: none"> -Reduce equipment's life -Increase cable losses -Inject more harmonic current -phase faults -Poor inverter efficiency
 <p>Fluctuation</p>	<p>Voltage changes up Or down from its rated supply voltage</p>	<ul style="list-style-type: none"> -Using equipment or devices that require a higher load. -Repeated On/Off of electrical motors -Oscillating loads 	<ul style="list-style-type: none"> -Changes in torque and slip motors -Harmful to household appliances and electronic appliances of MGs -Lights flicker or glow more brightly
 <p>Harmonics</p>	<p>The distortion of current or voltage sinusoidal waveform than is pure sinusoidal shape because of the harmonics</p>	<ul style="list-style-type: none"> -Nonlinear loads -Electronic inverter -Computer drives -Variable speed motors 	<ul style="list-style-type: none"> -Reduces performance of energy generation in MG's units -Distort the MG's output AC sine wave -Inefficiencies in equipment operations and overheating

PQ problem	Brief Description	Causes	Effects
			-Higher line losses ($I^2 \cdot R$).
	The distortion of voltage and current waveforms with a frequency range from 2 to 150 kHz	-Switching of power electronics devices, especially inverters -Modern sources	-Inverter instability for MG units -Lost connection with smart meter -Increase power losses -Failures in protection devices -Damaged power supply

However, MG sources rely heavily on power electronics components like converters. Supraharmonic (SH) emissions are a novel phenomenon that results from high-frequency emissions. SH emissions are defined as the introduction of harmonics into a system by grid devices with a frequency range of 2-150 kHz [5]. A growing number of power electronic interfaces containing components like heat pumps, electric cars, DC/AC converters, and PV systems charge controllers have prompted concerns about emissions in this frequency range [5]. Recently, certain standards and regulations covering various concerns linked to the integration of technological challenges and PQ issues are thoroughly researched and discussed in the literature [7] - [15].

1.6. Research Objectives

IEEE Standards describe voltage sag as a brief drop in the RMS voltage at a particular location in the electrical system below a certain threshold. The application will determine which threshold to use. The word ‘sag’ can be used to refer to the concept ‘voltage sag’ because the meaning of the term ‘sag’ is clear from the context [8]. PQ issues are an important subject in sustaining power grid development and effective power systems performance standards, according to the literature ([1]–[6]). The voltage level stability at load buses is one of these issues that should be taken seriously. Low voltage (LV) level preservation at consumer common point

connections is what the terms voltage sag and voltage swell refers to. It would be far from justified to assert accurate assessment for PQ concerns and, therefore, quality improvement in power systems with MGs without establishing the consequences of these variations on the performance of power grids. So, the present study aims at:

1. Specifying the role of MGs with solar PV in PQ problems of LV distribution networks.
2. Identifying the margin of voltage deviation in a proto-type LV system in order to assess the severity of voltage sag in it.
3. Determining the contribution size of the solar PV unit in the voltage level issue.
4. Verifying the optimum PV unit location inside an MG for best voltage sag mitigation.

1.7. Thesis Structure and Organization

The study consists of five chapters: Chapter one tackle the introductory concepts that include visualizing the problem statement and the objectives adopted

The second chapter deals with the literature survey and shows the research tackled the same topic. In this context, the works of several authors were shown, and their contribution was remarked on as well as identifying the research gap. Chapter three represents the research methodology. Load flow analysis is conducted by using the modified Newton-Raphson iterative method. This method is carried out through a modern simulation package specialized in power systems. Chapter four is about an LV distribution network with real data specified, and the simulation process is visualized. The results for power system performance are then presented. The results are discussed, and the study ends with some conclusions in chapter five.

CHAPTER TWO

OVERVIEW OF VOLTAGE STABILITY IN LV NETWORKS

2.1. Voltage Stability

Voltage stability seems to be a power system's ability to sustain constant passable voltages throughout all system buses under usual operation conditions and after a disruption. Voltage control would be an essential component of power system stability in the power systems Eco system [16].

In recent years, voltage instability has been responsible for several major network collapses in many places worldwide. The following were certain causes of voltage stability issues in power systems:

- In a largely stressed power system, a huge load or a huge disruption.
- There is a significant disruption among generation & loads.
- unfavorable load properties.
- The greater distance between the voltage source and load center.
- Source voltage too low.
- There isn't sufficient load proportional compensation.
- ULTC operation under low voltage conditions.
- Inadequate coordination among different control and protection systems.
- At heavy loads, reactive power is consumed highly.
- FACTS controllers in inappropriate places.

Voltage stability can be divided into two broad categories:

A) Large disruption voltage stability: This would be described as the power system's ability to sustain steady voltages in the face of large disruptions like system faults, load lost opportunity or generation absence. Large

disturbances voltage stability can be categorized into two categories. a) Temporary Stability, b) Long-term Stability.

B) Minor commotion (Weak signal) small disruption in voltage stability was concerned with a system's ability to control voltages following small perturbations, such as a gradual change in load, this type of Stability can be studied with steady-state approaches that use linearization of the system dynamic equations at a given operating point.

Voltage stability is considered the main issue among the PQ issues, as shown in Figure (7).

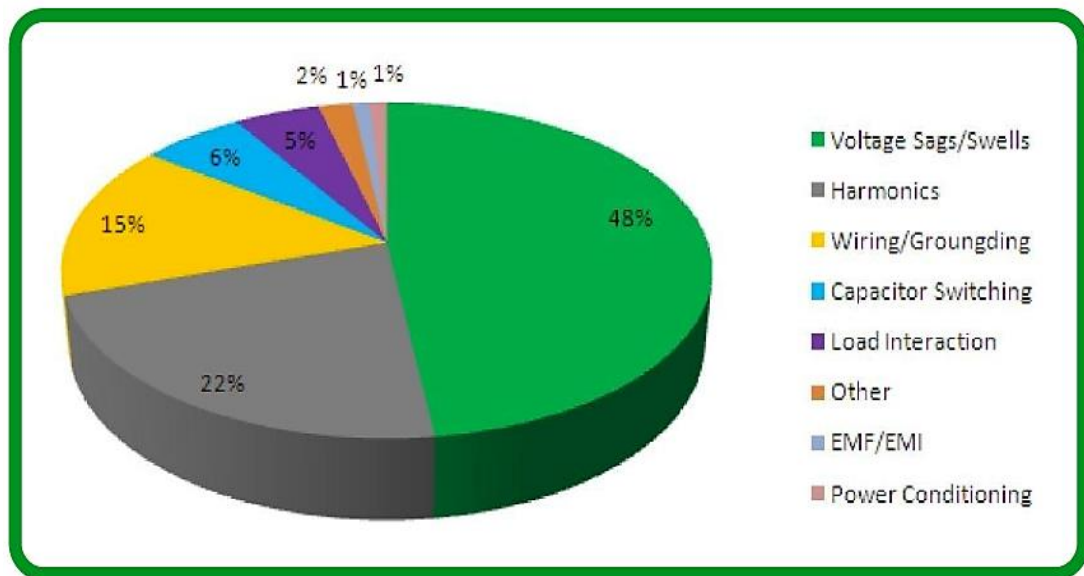


Figure 7. Comparative overview of PQ issues contribution in power grids

That should justify the need for mitigation techniques that would manage to keep the voltage level within the specified limits defined by international standards.

2.2. Mitigation by Custom Power Devices (CPD) Techniques

The critical problem with power quality is voltage stability, which necessitates regulatory. Voltage organization has been primarily influenced by the reactionary balance of power and the excitement system's duration consistent. The normal distributions of PQ problems by period reveal which disorder that will last less than one second exceeds the number of others in terms of occurrence. Like those

characterized by IEEE and IEC, Norms were presented to identify PQ; [7]-[15]. DG, in conjunction with MGs, could indeed result in relatively clean and more accessible power when incorporated with renewable technologies like solar and wind. Electric power system technicians frequently attempt to maintain power quality and employ CPDs with various techniques, as illustrated below.

2.2.1. Using one CPD

Many researches [16] – [22] examined using a single CPD to mitigate voltage quality, or PQ in general, in LV distribution networks. In Ref [16], the authors tried to improve PQ and harmonics distortion mitigation using a developed control scheme for DSTATCOM. Their results show the effectiveness of DSTATCOM for the harmonic reduction in distorted current and the validity and flexibility of the proposed scheme. The DSTATCOM configuration, as shown in Figure (2-1), uses a voltage source converter (VSC) supplied from a DC source to inject compensating voltage into the sensitive load to correct for the faulted voltage via an injecting transformer.

Distortion mitigation using a developed control scheme for DSTATCOM. Their results show the effectiveness of DSTATCOM for a harmonic reduction in distorted current and the validity and flexibility of the proposed scheme. The DSTATCOM configuration, as shown in Figure (8), uses a voltage source converter (VSC) supplied by a DC source to inject compensating voltage into the sensitive load to correct the faulted voltage via an injecting transformer.

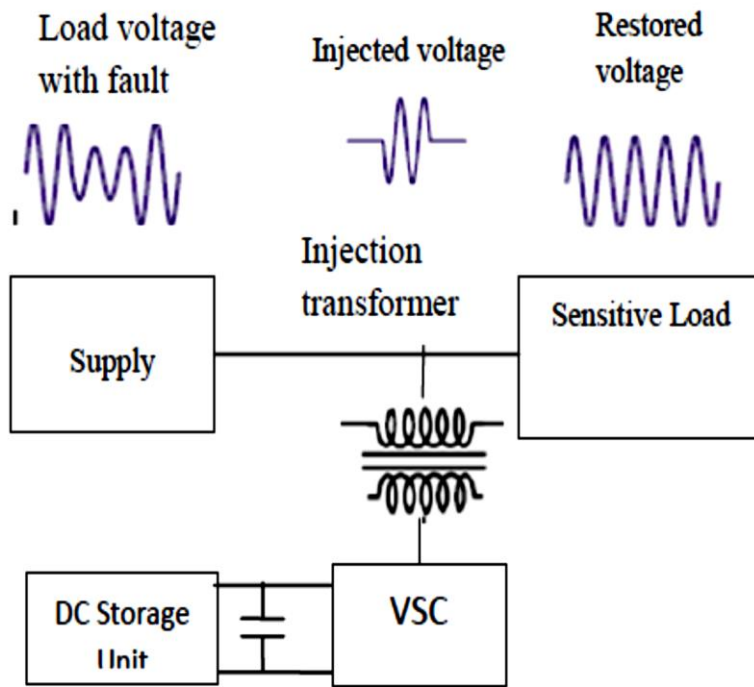


Figure 8. Distribution Static Synchronous Compensator (D-STATCOM)

In Ref [17], the authors demonstrate the design of PV-fed UPQC to mitigate PQ. UPQC, as shown in Figure (9), Has two main kinds of Active Power Filters (APF). The shunt APF will be the first, and the sequence APF will be the second. The shunt APF handles current-relating issues, while the series APF handles voltage-relating issues.

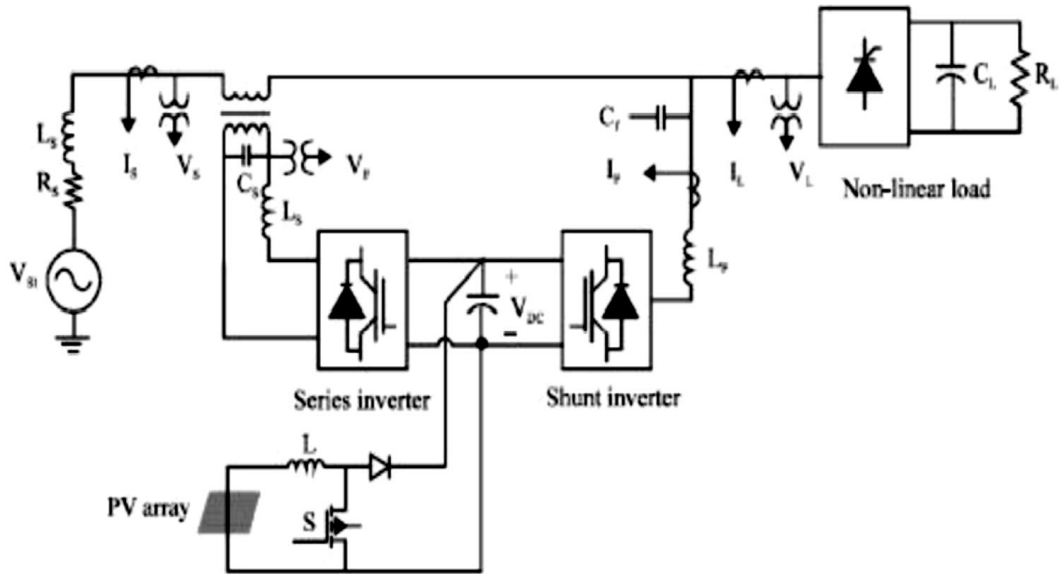


Figure 9. Block diagram of PV fed UPQC

The suggested UPQC-PV will have supplied an advantageous method for mitigating voltage and harmonic currents.

To recompense for voltage sags, the researchers of Ref [18] suggested a Series Voltage Regulator (SVR) for a distribution converter. The experimental find out showed voltage sag and swell recompense in the absence of a direct current link and related electrolytic capacitors. Figures (10) depict the suggested distribution converter with a power electronics module conceptual scheme.

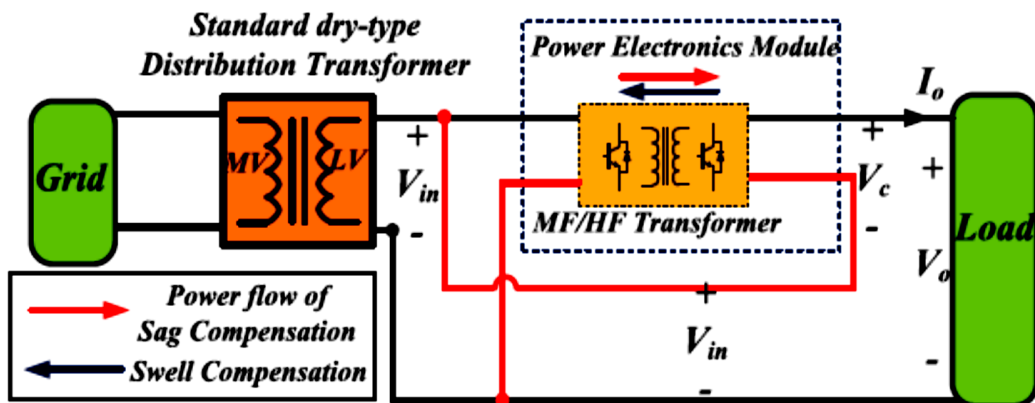


Figure 10. Conceptual scheme of the proposed distribution transformer with power electronics module

In Ref [19], The utility included in DVR in distribution networks for voltage sag and swell reduction is demonstrated. The schematic view of the DVR is shown in Figure (11).

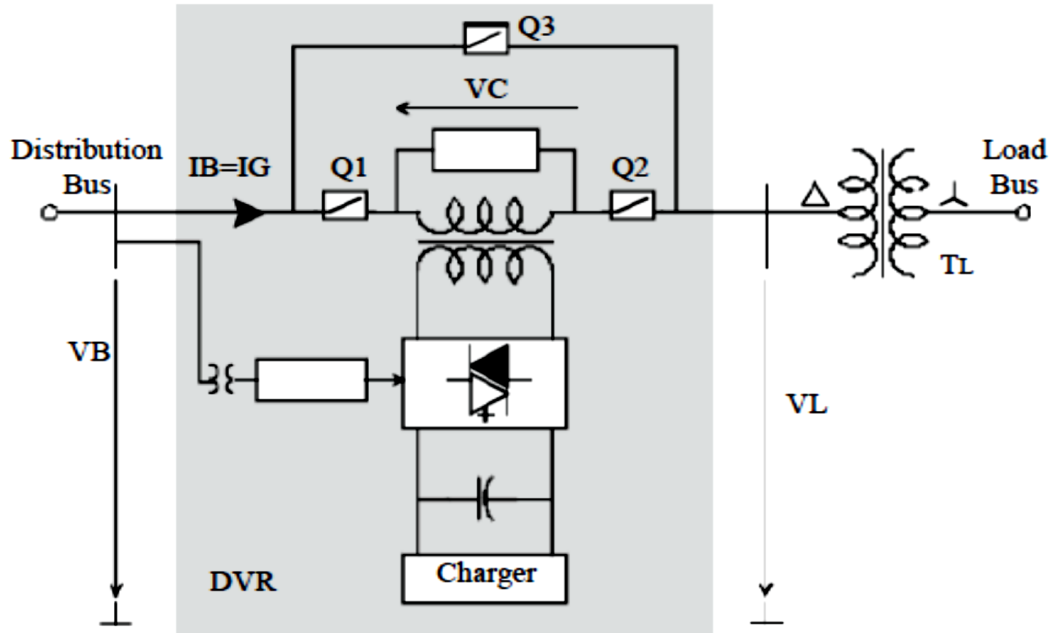


Figure 11. Schematic diagram of the DVR

The findings demonstrate that DVR efficiently needs to compensate for sag/swell, offers better voltage organization, and improves power system performance. The verification by the experimental system shows very good performance compliance with analysis and simulations. In Ref [20], A new DVR structure with a crossbred control technique of grid voltage feed-forward as well as load voltage has been suggested. Figure 1 depicts the new DVR structure (12). The storage battery would be highly centralized for saving energy in this setup, and the storing energy has been the outcome via the integration of various transformers and a number of winding transformers.

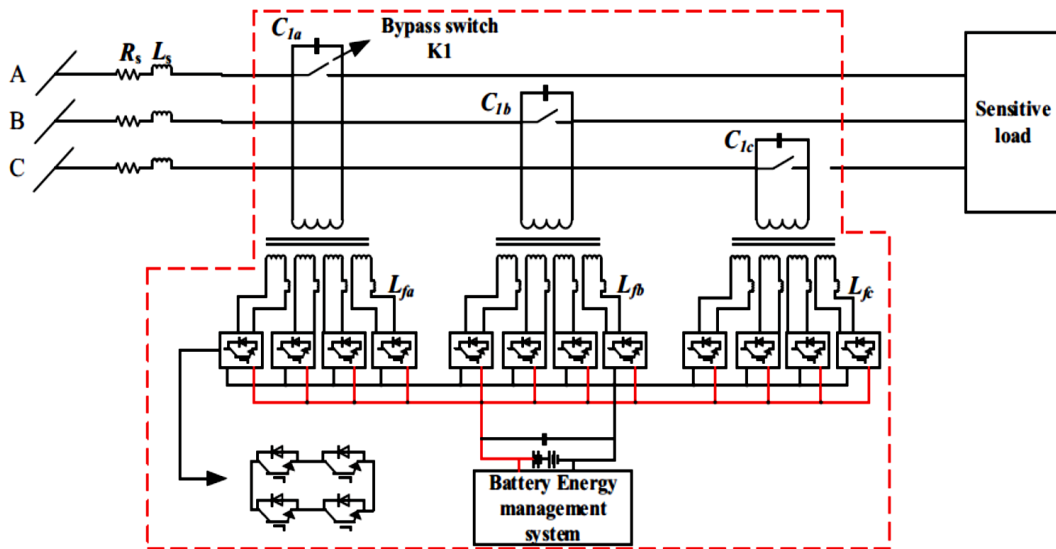


Figure 12. The New DVR topology diagram

The results demonstrated that the improved DVR compensates for the elevated harmonic components of the load voltage. In Ref [21], improving PQ by using a "Shunt Active Power Filter" (APF) is suggested for grid-connecting PV generation systems. The schematic diagram of the proposed system is shown in Figure (13).

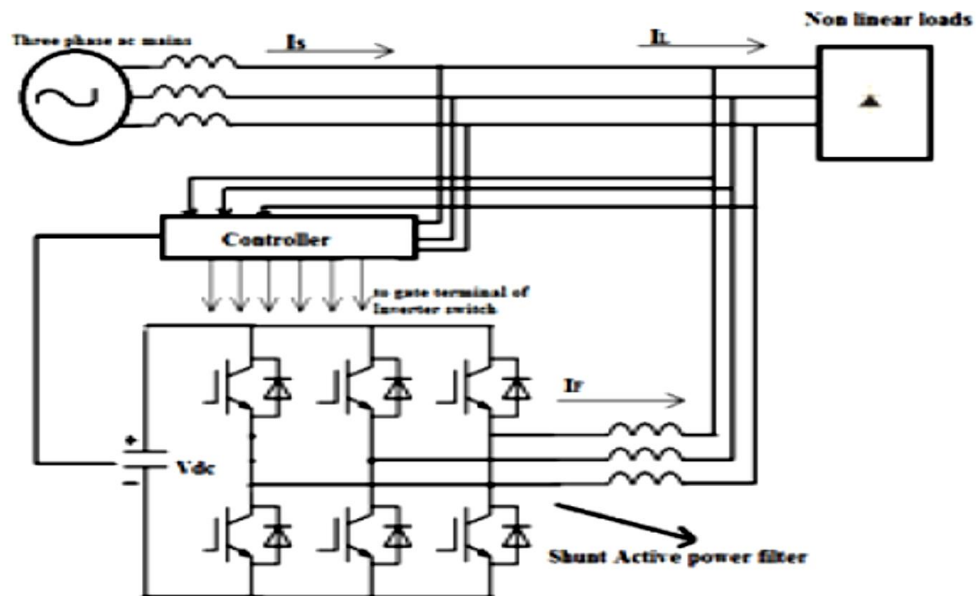


Figure 13. Shunt Active Power Filter (SAPF)

The findings demonstrate that such a maneuverer active filter outperformed a passive filter, which could interfere with the effectiveness of the reciprocal process. Furthermore, maneuverer, active filters reduce the total harmonics generated by non-linear loads and improve the power component effectiveness.

In Ref [22], the design of a Superconducting Shunt Resonator (SSR) for voltage sag mitigation, whose schematic diagram is shown in Figure (14), was proposed. SSR's fundamental topology consists of a static switch, a superconductors coil (SC), a capacitor, and a Metal Oxide Varistor (MOV). To form an LC resonant frequency circuit, the SC has been connected in parallel with a capacitor and tuned at a power frequency (50 Hz or 60 Hz). Thus, when working normally, the inductance of the SSR is infinite, and electric power could be saved in the device as magnetic energy or electrostatic energy.

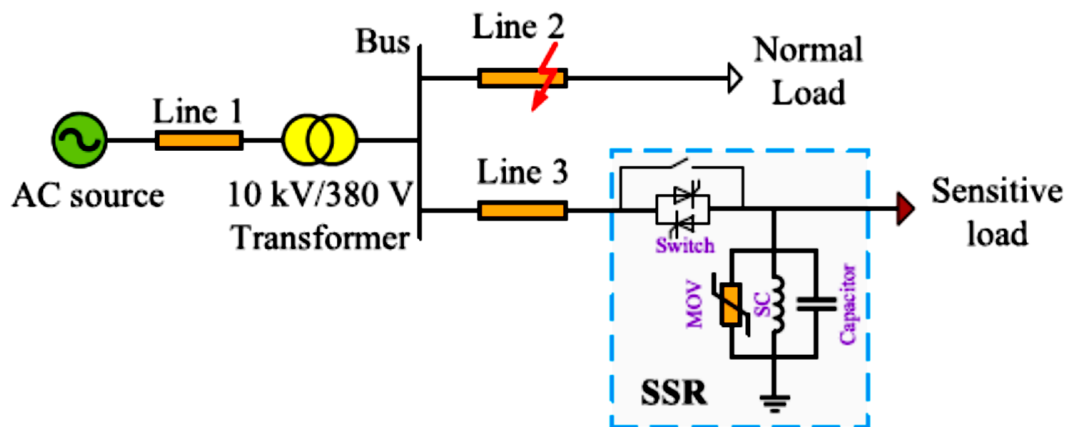


Figure 14. Principle of the proposed SSR

The topology and monitoring compilation are substantially reduced in comparison to the DVR. Furthermore, because fewer power electronics switches are used, the expense of SSR has been substantially decreased. Furthermore, the device's AC losses have been significantly reduced because of the SC. Once voltage sag takes place, the static switch is deactivated, and the responsive load is powered directly by the SSR. Figure (15) depicts the LC resonance circuit's natural dissipation characteristic.

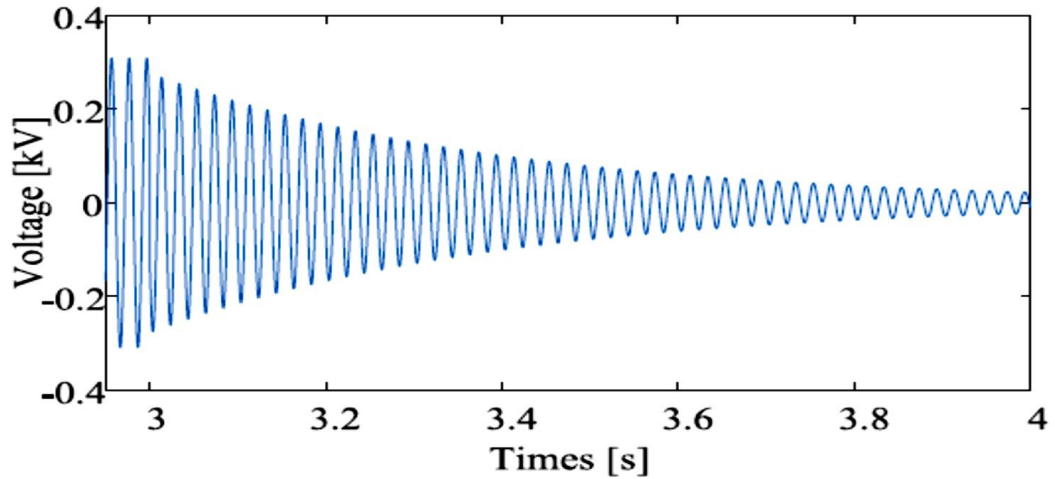


Figure 15. The LC resonant frequency circuit's natural decomposition properties

Table (2) shows the comparison table of these mitigation techniques and their details.

Table 2. Literature review comparison for single CPD

Study	Title	Objectives	Methodology	Main Results	Limitations
Montaserbillah Hafez, et. al. 2019 . [4]	Voltage Sag Enhancement in Microgrid with Applications on Sensitive Loads	Using PLC to insert or remove Thyristor Switched Capacitors	ETAP	Thyristor Switched Capacitor control for mitigation of voltage sag in nuclear research reactor as a sensitive load	This research was applied using only one CPD.
Ahmed M. Hassan, et. al. 2014 . [5]	Modeling and Simulation of Integrated SVC and EAF using MATLAB & ETAP	Using Electric Arc Furnace as a non-linear load with SVC simulated for V sag mitigation	MATLAB & ETAP	Combination of ETAP and MATLAB simulation was implemented to verify real time response for V sag mitigation	This research was applied using only one CPD.

Study	Title	Objectives	Methodology	Main Results	Limitations
S. Singh, et.al. 2015 . [6]	The Role of DSTATCOM as Active Filter to Mitigate Harmonics in Distribution System	-to improve PQ and harmonics distortion mitigation -includes the developed control scheme for DSTATCOM.	MATLAB SIMULINK	-results show effectiveness of DSTATCOM for harmonic reduction in distorted current and validity and flexibility of the proposed scheme	This research was applied using only one CPD.
P. M. A. Dass, et. al. 2016. [7]	“Voltage Sag and Harmonic Compensation of PV Fed Unified Power Quality Conditioner”	demonstrates the design of PV fed UPQC	MATLAB SIMULINK	-The suggested "UPQC-PV" had supplied an advantageous method for mitigating "V & I harmonics".	This research was applied using only one CPD.
S.A. Sewan , et. al. 2017. [8]	“Series Voltage Regulator for a Distribution Transformer to compensate Voltage Sag/Swell”	Voltage organizer for a allocation converter that identifies power quality problems in a power distribution systems.	Experimental method	Experimental outcomes showed voltage sag and swell preparations in the upcoming grids without a "dc-link" and related "electrolytic capacitors".	This research was applied using only one CPD.
S. Estimably, et. al. 2018. [9]	“Mitigation Voltage Sag Using DVR with Power Distribution Networks for Enhancing the Power System Quality”	The utility of incorporating "DVR" into an allocation system as a means of "V sag and swell" reduction was demonstrated using operation strategy and regulation.	MATLAB SIMULINK	-"DVR" successfully need to compensate for "sag/swell", offers valuable voltage organization, and improves power system effectiveness. - Experimental system confirmation demonstrates very great performances submission with assessment and simulation models.	This research was applied using only one CPD.

Study	Title	Objectives	Methodology	Main Results	Limitations
Lungfu et al. 2019. [10]	“Compensation Strategy for Multiple Series Centralized Voltage Sag in Medium Voltage Distribution Network”	Presenting a crossbred "grid voltage feed" forward and load voltage regulation control strategy.	Simulation and experiment	The newly "DVR" structure could indeed greatly decrease the supplementary side of the converter's working present while still producing highly voltage. -A composite control method with better dynamic as well as stable state performance is suggested. -The novel "DVR's higher harmonic content of load voltage" compensation would be lesser.	This research was applied using only one CPD.
A. Bagi, et. al. 2020. [11]	“Power Quality Improvement using a Shunt Active Power Filter for Grid Connected Photovoltaic Generation System”	-improving the PQ of a grid connecting PV generation system's maneuver Activated Power Filter	MATLAB SIMULINK	-A shunt active filter seems to have a benefit above a passive filter, that might interfere with the effectiveness of the reparations on method. -a shunting active filter reduces the harmonic currents generated by non-linear loads and improves power factor quality	This research was applied using only one CPD..
A.S. Ying, et. al. 2012. [12]	“Circuit Principle and Design of Superconducting Shunt	-to safeguard sensitively equipment from voltage drops - can reduce" voltage swell"	Using Shunt Resonator	-SSR can store energy -SSR mitigates voltage sags. -SSR mitigates the transient	This research was applied using only one CPD.

Study	Title	Objectives	Methodology	Main Results	Limitations
	Resonator for Voltage Sag Mitigation”			voltage disturbances.	

2.2.2. Using multiple CPDs

Other research works, [23] – [26], examined using multiple CPDs to mitigate voltage quality in LV distribution networks. In Ref [23] – [26], the authors studied using DVR and DSTATCOM through comparative analysis to examine the most effective CPD. All these methods use MATLAB/SIMULINK to analyze the effect of mitigation techniques.

The simulation finding demonstrates that "DVR" seems to be more effective than "D-STATCOM" at improving PQ and reducing "voltage sag and swell" all through different faults on the LV network. The findings also suggest that the multilevel principle would be the better alternator for using limited frequency inverters with small output voltage variations. A comparative assessment was conducted in Ref [27] to identify the best reduction device between "D-STATCOM", "UPQC", "UPS", "TVSS", and "DVR". According to the findings of this study, transient seems to be the most serious power quality problem, accompanied by "voltage spike" and fluctuations. Power quality surveillance methods were discovered to be primarily used for surveillance harmonics, with "UPQC", "STATCOM", and rotating reserve being the most efficient CPDs. "STATCOM" has been determined to be a viable option due to its many advantages [27]. The insightful comparison between these methods is provided in Table (3).

Table 3. Literature review comparison for multiple CPDs

Study	Title	Objectives	Methodology	Main Results	Limitations
Kumar, et. al. 2011. [13]	“Voltage Dip mitigation in Distribution System by Using DSTATCOM”	PQ improvement using DSTATCOM & DVR	MATLAB simulation	DVR is more efficient than DSTATCOM in PQ improvement	This research was applied using only 2 CPDs.
Smriti Dey 2014. [14]	“Comparison of DVR and D-STATCOM for Voltage Quality Improvement”	V quality improvement by using DVR and D-STATCOM	MATLAB SIMULINK	-The simulation findings demonstrate that "DVR" seem to be more effective than "D-STATCOM" for improving PQ. -The multi-tiered alternator has been the better alternator for using lower frequency inverters with lower power voltage instability.	This research was applied using only 2 CPDs.
Vishwakarma, et. al. 2015. [15]	“Simulation and Comparison of DVR and DSTATCOM used for Voltage Sag Mitigation at Distribution Side”	- A comparative evaluation of "DVR" and "DSTATCOM" is described to learn why both equipment have effectively been implemented to power systems for controlling system voltage.	MATLAB SIMULINK	-simulations showed that DVR provides relatively better V regulation capability -The ability of "DSTATCOM" for power reparations and V organization is determined by the rating of the "dc storage device".	This research was applied using only 2 CPDs.
Rajeev, et. al.	“Comparison of Voltage Sag and	- two different	MATLAB	-more effective "DVR" perform	This research

Study	Title	Objectives	Methodology	Main Results	Limitations
2017. [16]	Swell Mitigation Using DVR and D-STATCOM “	methods of mitigating V sag and swell using two different CPDs: DVR and D-STATCOM and comparison of these two mitigation methods	SIMULINK	ance than" D-STATCOM" in minimizing V sag and swell all through numerous LV network problems -DVR efficiency in improving" V and I "quality	was applied using only 2 CPDs.
Hossian, et. al. 2018. [17]	“Analysis and Mitigation of Power Quality Issues in Distributed Generation Systems Using Custom Power Devices”	PQ supervision methods and potential solutions to PQ problems in power system applications have been thoroughly investigated.	Survey	- PQ supervision methods were discovered to be used for checking harmonics primarily - "UPQC and STATCOM "were discovered to become the most efficient "CPDs". -"STATCOM" may be a viable option due to the benefits it provides.	

2.3. Mitigation by Strategical Planned Techniques

Some authors [28] – [31] suggested real strategic techniques for mitigating voltage disturbances in LV distribution networks. Over voltages and voltages, misbalance reduction in areas with high "RES" penetration is described in ref [28]. The modified three-phase damping control strategy has been used in the technique. As a result, various control methods have been carried out to confirm the effect on the voltage level at residences. The findings demonstrate that now the adapted dampers control strategy seems to be superior to the positive-sequence control strategy with PF and the drooped positively sequence control method for areas with higher penetration of “RES” and PQ troubles. PQ evaluation of grid-connected PV system has been

validated in Ref [29] to investigate voltage sag, flicker, harmonics, voltage unbalance, and harmonic distortion per the current integration requirement. In Ref [30], the system voltage sag has been reduced by utilizing distributed energy resources “DER”. It proposed a novel structure for active and reactive planning of transformer “DERs” to address voltage-sag issues. The system size has been doubled and quadrupled in comparison to the IEEE 33-bus system, and the optimal solution's computational time has risen by 16.7 per cent and 30.85 per cent, respectively. Furthermore, the voltage-sag issue was effectively solved using modularity-based fragmentation and ZCI priorities. Ref [31] presents a method to assess bus and grid structure based on voltage sags/swells using voltage ellipse variables. The simulation results showed that the technique is accurate and viable.

Table 4. Literature review comparison for strategical planned techniques

Study	Title	Objectives	Methodology	Main Results	Limitations
V. Bozalakov, et. al. 2019. [18]	“Overvoltage and voltage unbalance mitigation in areas with high penetration of renewable energy resources by using the modified three phase damping control strategy”	To confirm the effect on V level at residential areas, a comparison of various control methods has been done. .	Testing control strategies by simulation procedures	-When comparing to the positively sequence control method with PF and drooped favorable control method, the adapted dampers control method is more ideal for application with growing penetration of renewable energy resources and power quality issues.	Strategical viewpoint
Ali Q. Al-Shetwi, et. al. 2020. [19]	“Power Quality Assessment of Grid-Connected PV System in Compliance with the Recent Integration Requirements”	to look into last several integrations need such as "V sag, V flicker, harmonics, V unbalance, and harmonic distortion"	Simulation	This research can help the development of gentle "PVPP" integration by optimization design, operation, and controlling methods for elevated PQ and green electricity.	Strategical viewpoint
Ahmed Mustafa, et. al. 2021. [20]	“System Level-Based Voltage-Sag Mitigation Using Distributed	proposes a new framework for active/reactive power	A network partitioning algorithm based on	-System size has been doubled and quadrupled when tried to compare to the" IEEE 33-	Strategical viewpoint

Study	Title	Objectives	Methodology	Main Results	Limit ations
	Energy Resources”	management of inverter based DERs to mitigate voltage-sag problems in ADSs	voltage sensitivity analysis	bus system”. - Computational time for the optimization process has been risen by 16.7percent and 30.85 percent, respectively. -The voltage-sag issue was effectively solved using modularity-based fragmentation and ZCI priority setting.	
A.S. Lima, et.al. 2012. [21]	“An Evaluation Method for Bus and Grid Structure Based on Voltage Sags /Swells Using Voltage Ellipse Parameters”	On critical loads, "V sags and swells". -to assess the bus and grid structure utilizing voltage ellipse variables based on "voltage sags/swells"	Simulation	The findings of the simulation demonstrated that the method seems to be accurate and viable. .	Strategical viewpoint

CHAPTER THREE

ANALYSIS OF DISTRIBUTION SYSTEM WITH SOLAR PV

3.1. Solar PV Basics

3.1.1. Solar Cell Principles

The solar cell is the basic unit of a photovoltaic module and is responsible for transforming direct sunlight or photons into electrical energy. The solar cell is made up of a "p-n" intersection formed in a thin layer of semiconductors, like that found in a "p-n" diode. Its operating properties are like those of a "p-n diode", and it has been affected by surface temp and solar radiation. A PV cell could be patterned as a current source to characterize its electrical characteristics; if no sunlight was available to generate current, the Photo voltaic cell behaves like a diode. The Photovoltaic cell generates current as the intensity of incoming light rises.

3.1.2. Solar Cell Electrical Equivalent Circuit

A double or single-diode model could indeed undertake the solar cell's equivalent electrical circuits. The single-diode equivalent model would be both simple and reliable. Figure (16) depicts a single-diode tantamount circuit with series and parallel contact resistance

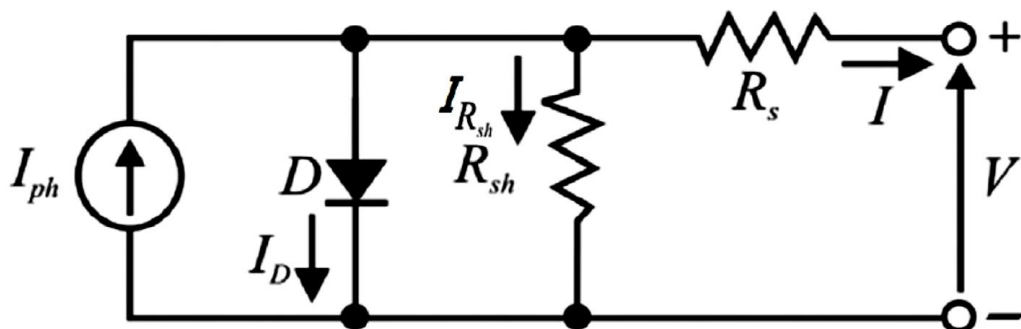


Figure 16. Equivalent circuit of the single-diode solar cell

For a single-diode equivalent circuit, the relationship between the delivered current (I) and the delivered voltage (V) is as follows.:

$$I = I_{ph} - I_D - I_{R_{sh}} \dots\dots\dots (1)$$

$$I = I_{ph} - I_0 \{ \exp[q(V + I.R_s)/(AKT)] - 1 \} - (V + I.R_s / R_{sh}) \dots\dots\dots (2)$$

Solar cells made of Si and other semiconductor substances are categorized into two types:

1." Mono (Single) crystalline silicon", Mono-crystalline cells have been composed of a single command crystal of Si. Mono - crystalline effectiveness ranges between 15 and 20 per cent; however, it had the longest life span and was also the costliest.

2. Poly (multi) crystalline, which would be made up of atom groups, each with organized atoms (single crystalline) which vary from the others. Although poly crystalline cells have lower performance (13% -17%), they would be less expensive than monocrystalline cells.

3. Thin film with no constructional atom arrangement. Thin film Si cells can be utilized in many tiny consumer goods since they are inexpensive and have shorter lifespans and efficiencies than crystalline silicon cells.

3.1.3. Selection of Solar Module

Selecting and trying to order the proper modules would be a vital step in any photovoltaic solar project. Those who were also typically the most expensive component of the system and selecting the inaccurate product could be an expensive mistake. This selection must be guided not only by the performance, effectiveness, and expense but also by the operating conditions.

Many factors influence the choice of the kind of panel that should be utilized, including available space, surface type, weather, and investment costs. As a result, selection requirements must be utilized to choose Photovoltaic modules that have been suitable for the weather conditions in Iraq, like enhanced performance at

elevated temps at a minimal price. Poly-crystalline solar modules are used in this job because they have a reduced power temp coefficient and are highly efficient at a lower price. Table (5) displays a few brands of modules with (250 - 540) Wp maximum power ranges, as well as the main features of every type that will be accessible in the 2022 PV market. The Sun power "(SPRA450COM)" module was selected from the Table for this job, but it does have a better requirement in terms of type, power, expense, and guarantee, with the usual electrical properties of this PV module seen in Tables (5) and (6).

Table 5. Some brands of solar panel modules

MANUFACTURER	PANEL EFFICIENCY	TEMPERATURE COEFFICIENT	PRICE*	WARRANTY PERIOD
Sun Power	22.8%	-0.29	\$18.720 to \$22.440	25 years
LG	22.1%	-0.29	\$14.760 to \$20.280	25 years
REC	21.9%	-0.26	\$13.920 to \$18.600	25 years
Panasonic	21.7%	-0.26	\$14.640 to \$18.600	25 years
Q CELLS	21.4%	-0.34	\$13.020 to \$18.960	25 years
AXITEC	20.45%	-0.26	\$13,020 to \$16,980	25 years
SILFAB	21.4%	-0.36	\$14.700 to \$18.540	25 years

Table 5. (continued)

MANUFACTURER	PANEL EFFICIENCY	TEMPERATURE COEFFICIENT	PRICE*	WARRANTY PERIOD
Solaria	20.5%	-0.39	\$14.760 to \$18.240	25 years
Mission Solar	19.35%	-0.35	\$13.500 to \$16.140	25 years
LA Solar Group	20.6%	-0.37	\$14.100 to \$14.700	25 years
Canadian Solar	20.6%	-0.35	\$16.200 to \$19.200	25 years
Jinko Solar	21.33%	-0.35	\$13.500 to \$17.820	25 years

MANUFACTURER	PANEL EFFICIENCY	TEMPERATURE COEFFICIENT	PRICE*	WARRANTY PERIOD
Trina Solar	20.4%	-0.36	\$13,860 to \$20,340	25 years

Table 6. SUNPOWER brand electrical data

AT standard test conditions								
Module	Platform (number of cell)	Nominal power	Power tolerance (%)	Rated voltage Vmp (V)	Rated current Imp (A)	Open circuit voltage Voc (V)	Short circuit current, Isc (A)	Max system voltage ULVmax (V)
SPR-A450-COM	72	450	+5/-0	44.0	10.2	51.9	11.0	1500
SPR-A440-COM*	72	440	+5/-0	43.4	10.2	51.6	10.9	1500
SPR-A430-COM	72	430	+5/-0	42.7	10.1	51.2	10.9	1500
SPR-A425	66	425	+5/-0	40.7	10.4	48.2	10.9	1000
SPR-A420	66	420	+5/-0	40.5	10.4	48.2	10.9	1000
SPR-A415	66	415	+5/-0	40.3	10.3	48.2	10.9	1000
SPR-A410	66	410	+5/-0	40.0	10.2	48.2	10.9	1000
SPR-A400	66	400	+5/-0	39.5	10.1	48.1	10.9	1000
SPR-A490	66	390	+5/-0	39.0	10.0	48.0	10.8	1000

3.2. PV System Layout

The design of big-scale solar PV systems would be a fascinating method which necessitates substantial experience and practical knowledge. The design should be optimized by considering the effect of the number of components, their kind and configuration inside the installation field, and the trade-off among the entire cost and correlating energy production of the Photovoltaic system.

Numerous design considerations impact the effectiveness of Photovoltaic power. To obtain the large quantities of energy, an effective design should enhance every variable. These variables involve climate information, soiling variables, shading variables, Photovoltaic technology performance properties, tilt and azimuth angles, different seasons snowpack, array incompatibility, inner leakages, and inverter efficiency.

3.2.1. PV Inverters Topologies

This portion examines the fundamental laws and characteristics of big-scale grid-connected Photovoltaic power station configurations, design, and layout. Grid-connected solar converters are categorized based on the following:

Topologies of structure,
AC power supply kind,
"DC-DC" converter type,
multilevel & bridge topologies.

The most significant were indeed structure topologies. In largely PV systems, the linkage of Photovoltaic inverters takes into account four basic topologies, as seen in Figure (17), that are:

1. Central Plant Inverter: Figure (17-a) depicts the central topology, whereby one inverter helps connect large numbers of solar modules. To produce higher voltage, the Photovoltaic modules are split into a series of connections recognized as strings, and these strings have been connected in parallel to start generating high power. The central inverter structure remains the preferred structure for large and medium-sized Photovoltaic system.

2. A single string of Photovoltaic modules was connecting to the inverter in the string inverter topology, which is depicted in Figure (17-b). This topology seems to be a condensed form of the central inverter. The architecture of inverter offers minimal losses, which increases energy production and improves power quality.

3. Multi string Plant Inverter: The multiple string inverter topology, which would be a refinement of the string inverter in which numerous strings are connected with their respective "DC to DC" converters to a unified "DC to AC" inverter, is depicted

in Figure (17-c). Each string could be separately regulated. The multi-string inverter can be used with PV plants ranging in size from 3 to 10 kilowatts.

4. AC Module (Module Integrated Technology): The AC module topology is shown in Figure (17-d), wherein a PV module and an inverter are combined into a single electrical unit. The mismatched losses among Photovoltaic modules are eliminated; however, the cost and complexity go up.

The right topology should be chosen based on factors including position, output power, effectiveness, expense, and dependability. The fundamental qualities take into account flexibility, "MPPT efficiency", dependability, and durability. The basic features of each topology vary depending on the power rating, quantity of Photovoltaic inverters, and quantity of Photovoltaic strings. For example, the centralized topology had lower "MPPT" efficiency, flexibility, and dependability than other topologies; however, stronger durability.

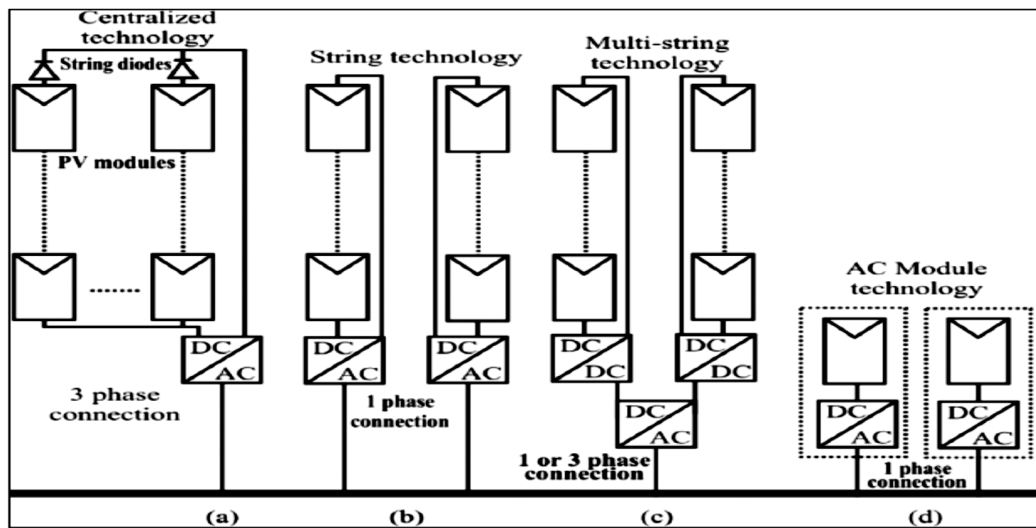


Figure 16. Types of PV inverters (a) central, (b) string, (c) multi-string, and (d) module inverter.

Miss matching, switching, "ac and dc" losses, shade, cloud cover, dust, cooling, and "MPPT" efficiency are all factors in power dissipation. The central topology in this situation exhibits significant mismatched loss. Given that several strings were coupled in parallel, central inverters suffer from exceptionally high inefficiencies on the "DC" side. In comparison, the central inverter's ac loss was minimal since the converter was linked to the inverter relatively closely.

Voltage balancing, “DC” and “AC” voltage changes, and power quality all have an impact. Due to the several strings being in parallel connection, the dc voltage variance was particularly significant in the case of centralized topology. Additionally, because there was only one inverter, the "ac voltage" variance was minimal and the voltage balancing was higher.

When numerous inverters are linked in parallel, like in the case of an integrated module, the voltage was unstable in particular. Components, installation, upkeep, land costs, and cable lengths on the “DC” or “AC” side are all included in the price. In comparison to other topologies, it could be said that the central topology seems to have the following benefits: resilience, low ac power dissipation, minimal "AC" voltage volatility, and fair installation and maintenance costs. String and multi-string topologies have many appealing general properties; however, as the number of inverters rises, the installation and maintenance costs become more and more prohibitive. The central inverter topology was selected for constructing a megawatt Photovoltaic plant using one of the megawatt central solar inverters after carefully considering the four topologies, with cost being the most relevant factor. According to comprehensive analysis and comparison of current inverter datasheets, the following minimal needs for inverters have been presumed:

1. Have a voltage output of 3-phase 400 Volts AC that is similar to the 50 Hz, national grid in Iraq.
2. Efficiency of 97% or more.
3. It's also required to have a "Maximum Power Point (MPP)" tracker available.
4. Should not have a minimum "DC input voltage of 1000 Volts".
5. Protection from lightning, over-voltage, and islands.
6. Adherence to global safety rules.

3.2.2. System Design

The primary system design is carried out using the generated power (1MWp), which was at the "0.4 kV AC" voltage level from the Photovoltaic. One step-up distribution converter with a 50Hz, 1250 KVA rating and output synchronized with the national grid raised the voltage from 0.4 kV to 11 kV.

The following formula is used to determine the photovoltaic modules in a string:

- The solar inverter's maximum "DC input voltage" is determined.
- The design could be created at the selected site in the coldest daytime temps with the greatest modules for each string.
- The relationship could be used to compute the different operational voltages at the highest and lowest site temps.

$$V(t) = V_{(25^\circ)} \times (1 + \alpha_v (T_m - T_{STC})) \dots\dots\dots (3)$$

The maximal number of modules in each string has been computed using equation (2):

$$\text{Maximum No. of modules/string} = \frac{(V_{max})_{inverter}}{V_{oc (T_{m.min})}} \dots\dots\dots (4)$$

Also, the minimum number of modules per string can be found using the following relation:

$$\text{Minimum No. of modules/string} = \frac{(V_{mpp})_{inv.min}}{V_{mpp (T_{m.max})}} \dots\dots\dots (5)$$

The following relationship can be used to determine the total number of parallel strings given the required power (1MWp).

$$\text{No. of strings in parallel} = \frac{(P_{output kW})_{inverter} / \eta_{max}}{(No.ofmodules/string) \times (P_{max})_{module}} \dots\dots (6)$$

3.2.3. PV Array Configuration

Because of inter-row shadowing and decreased diffusing irradiance in closely spaced arrays, major commercial Photovoltaic systems may regularly and predictably suffer wasted energy. Row spacing was chosen by making a compromise between limiting the plant's overall size, reducing inter-row shadowing, shortening cable runs, and reducing ohmic losses. From dawn to dusk, inter-row shadowing could never be completely eliminated.

The angles that must be considered when designing Photovoltaic plants can be seen in Figure (18). When determining the distance among Photovoltaic modules rows, the following angles should be put into an account in estimations.

The equation for the angle α of the rising sun:

$$\sin(\alpha) = [\cos(\phi) \cos(\delta) \cos(\omega) + \sin(\phi) \sin(\delta)] \dots\dots\dots (7)$$

Where:

$$\delta = 23.5 \sin [360/ 365 (J + 284)] \quad (\text{in Degree}) \dots\dots\dots (8)$$

As the globe spins on its axis at a rate of 15° each hour, the hour angle, or the angular displacement of the sun's east direction of the local meridian, could be computed as follows:

$$\omega = 15 (12 - ST) \quad (\text{in Degree}) \dots\dots\dots (9)$$

The azimuth angle γ is calculated from the relationship:

$$\cos \gamma = [\sin(\alpha) \sin(\phi) - \sin(\delta)] / \cos(\alpha) \cos(\phi) \dots\dots\dots (10)$$

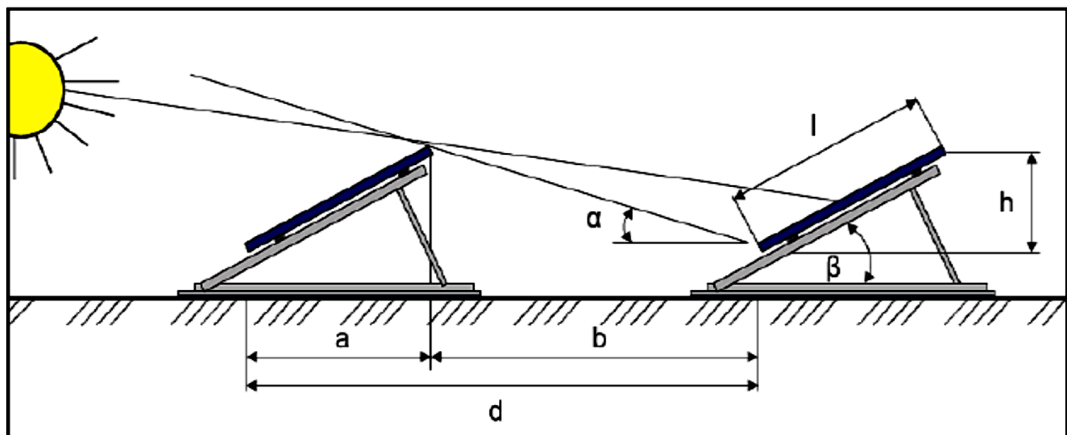


Figure 17. Calculating the distance between Photovoltaic modules rows

The ground coverage ratio (GCR), in which (l) is considered the length of the array and d is the spacing between rows, is the ratio of PV modules area to overall land area and calculated as follows:

$$GCR = \frac{l}{d} \dots\dots\dots (11)$$

The benefit of a shorter d and higher "GCR" array is that it produces more power density in (kWh/m²) than a similarly rated array with a longer row to row spacing and less inter-row shading loss, but it produces less overall energy.

3.3. Performance Analysis with solar PV

To carry out a performance analysis to the LV distribution network with solar PV, the following procedure is followed:

1. Get the single-line diagram (SLD) for the selected network.
2. Tabulate the network data for all the components (transformers, bus bars, cables, transmission lines, loads, and renewable energy sources).
3. Define the base quantities for the network (base impedance, base kV, base MVA, and base current).
4. Convert the network data to per-unit quantities using the following formula:

$$P. U. \text{ quantity} = \text{Actual quantity} / \text{Base quantity} \dots\dots\dots (12)$$

5. Define the slack bus, the generating bus, and the load buses.
6. Specify the lumped loads from the other passive loads at the load buses.
7. For modelling the PV generating unit, specify the following data:
 - The type and ratings of the solar panel
 - The number of panels included in the series in a single string.
 - The number of strings connected in parallel.
 - The type and ratings of the inverters used.
 - The type and ratings of the step-up transformer used to tie the PV unit to the network.
8. Apply the Load Flow Analysis according to Newton-Raphson Iterative Method [32].

3.4. Modeling & Analysis using Software ‘ETAP’

In this software, the following tasks could be performed through system modelling:

- Create and edit one-line diagrams
- Approve or deny information modifications.
- Geo Tagging - position of the equipment
- Intelligent connection, such as Automatic Insert
- Sub - systems designs that are layered

The details of such facilities are given in Appendix A.

CHAPTER FOUR

ANALYSIS AND CALCULATIONS

4.1. Solar PV System Design

4.1.1. Design Calculations by “PVSYST” Software

PVSYST is a photovoltaic software specialized in design of solar PV systems projects. In this section, the site geographical data as well as the total overall power output are given as input data to the software. The system specifications are determined as outcome results. These are shown in Tables (7) and (8).

Table 7. PV project summary by PVSYST

Geographical Site	Latitude	Longitude	Altitude	Time Zone	PV Field Orientation	Tilt/Azimuth
Al Mansur, Iraq	33.32° N	44.36° E	50m	UTC+3	Fixed plane, No shadings	33 / 0 °

Table 8. PV Project layout by PVSYST

PV Array modules	Total PV Power	Inverter units	Inverter Power	Produced Energy	Specific production	Perf. Ratio
4545 units	2000 kWp	18	1620 kW ac	3327 MWh/year	1663 kWh/kWp/year	81.80 %

The PV system outcome as given by PVSYST for the PV array, inverter, and electrical energy expected to be generated, are as shown in Table (9).

Table 9. PV system characteristics

PV module		Inverter	
Manufacturer	Generic	Manufacturer	Generic
Model	FS-6440-P Oct2020	Model	SP 100 000
Unit nom. Power	440 Wp	Unit nom. Power	90 kW ac
Number of modules	4545	Number of inverters	18
Nominal (STC)	2000 kWp	Total power	1620 kW ac
Modules	1515 x 3 in series	Operating voltage	420-800 V
P mpp @50°C	1838 kWp	P nom. Ratio (dc:ac)	1.23
U mpp @50°C	504 V		
I mpp @50°C	3648 A		
PV area	11453 m ²		

Furthermore, the electrical energy yield by the system is given as well. Figure (19) shows the Normalized productions (per installed kWp), and Figure (20) shows the Performance Ratio PR.

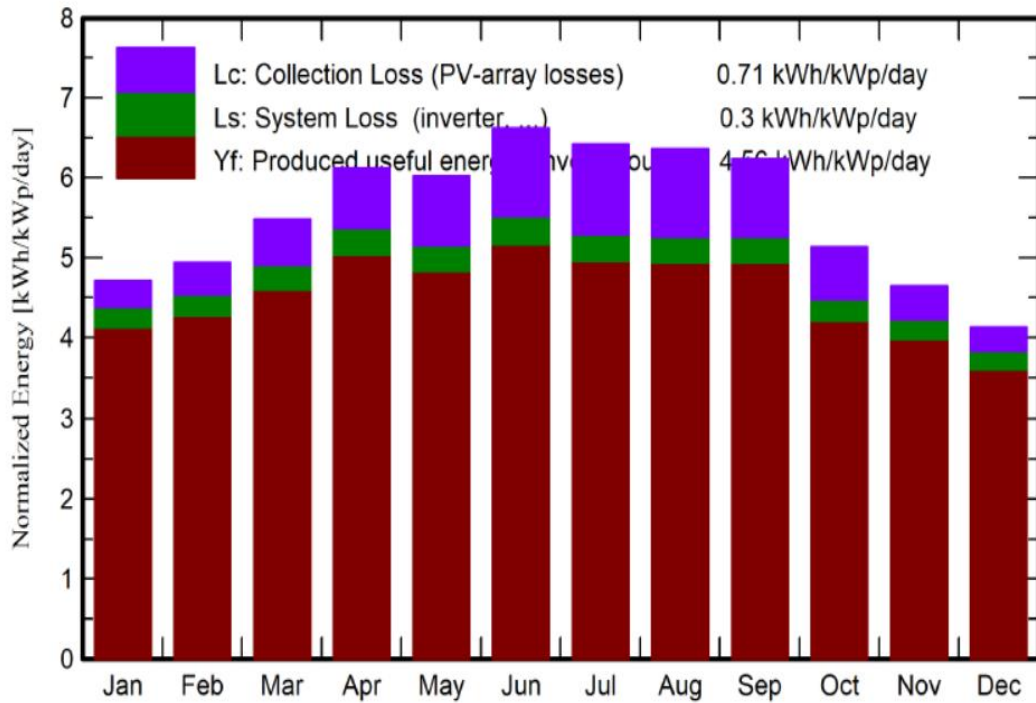


Figure 19. Normalized productions (per installed kWp)

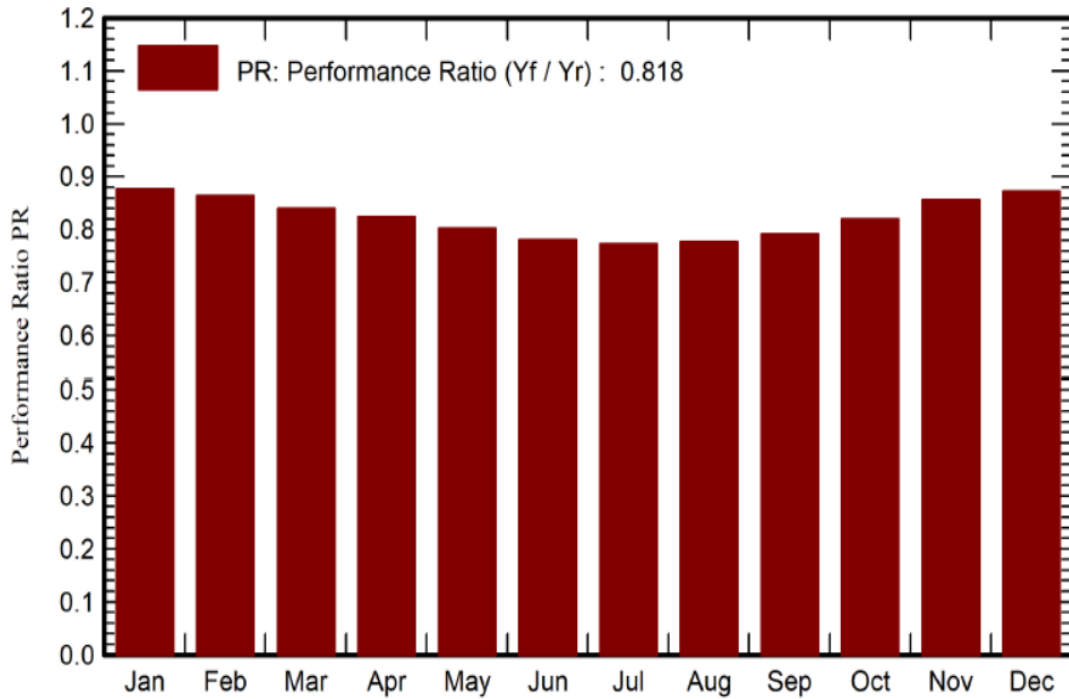


Figure 20. The Performance Ratio PR

4.1.2. Calculations of PV System Using Design Equations

A. Selection of PV module:

The main system design is undertaken based on the amount of generated power (2000kWp), the generated output power from the PV system is at 0.4 kV AC voltage level. It stepped up from 0.4 kV to 11 kV by a 2.5 MVA rated step-up transformer, the output of the power transformer is connected to the 11 kV grid.

The most recent available brands of solar PV modules rated more than 500W, are shown in Table (10), where the 540Wp module is selected for its higher power generated and relatively long lifetime.

Table 10. Brands and specifications of (> 500Wp) solar panels

Typical Type	520W	530W	540W
Max Power (P_{max})	520	530	540
Max Power voltage (V_{mp})	40.47	40.74	41.04
Max Power current (I_{mp})	12.85	13.01	13.17
Open circuit voltage (V_{oc})	48.99	49.26	49.53

Short circuit current (I_{sc})	13.53	13.69	13.85
Module Efficiency (%)	20.56	20.96	21.35
Max system voltage	1500V (DC)		
Max Series Fuse Rating	20A		
Temper. Coeff. of Voltage (α_v)	-0.29%		
Dimensions	2230×1134×35 mm		
Weight	28.9 kg		
Front glass	3.2mm tempered glass		
Output cables	4mm ² symmetrical length 1100mm		
Connectors	MC4 Compatible IP68		
Cell type	Mono-Crystalline PERC Half-Cell 9BB 182mm		
Number of cells	144cells		
Power tolerance	0±3%		

B. Inverter ratings:

PV inverter is selected according to the system rated power of 2 MW. This inverter consists of two units and has ratings as shown in Table (11).

Table 11. Solar inverter specifications

Max input power	2×1200 kW	Max AC output power	2×1000 kW
DC voltage range, mp	600V-800V	Nominal AC current	2×1445A
Max DC voltage	1100V	Nominal output voltage	400V
Max DC current	2×1710A	Output frequency	50/60Hz
Nominal AC output power	2×1000 kW	Harmonic current distortion	<3%
Power at $\cos\Phi=0.95$	2×950 kW	Power factor compensation	Yes

C. PV array configuration:

The number of PV modules in series per string is calculated as follows:

1. Maximum DC input voltage of the solar inverter is decided.
2. Maximum number of modules per string, the design can be made in the coldest daytime temperatures at the site location.

3. Operating voltages at the maximum and minimum site temperatures can be calculated using the relation:

$$V_{(t)} = V_{(25^\circ)} \times (1 + \alpha_v (T_m - T_{ST})) \quad (4-1)$$

Where:

$V_{(t)}$: Module output voltage at any temperature.

α_v : Temperature Coefficient of Voltage drop.

T_m : Module temperature in °C.

T_{ST} : Temperature at standard test conditions (25°C).

The maximum and minimum numbers of modules per string are calculated after determining the temperature range for climate in Iraq is chosen for worst case to be (-1°C) minimum, and (60°C) maximum. Hence, the operating voltages at this range are:

$$V_{oc(-1^\circ)} = 49.53 (1 + (-0.0029) \times (-1 - 25)) = 53.26 \text{ V}$$

$$V_{mp(+60^\circ)} = 41.04 (1 + (-0.0029) \times (60 - 25)) = 36.87 \text{ V}$$

Hence, the maximum number of modules per string is:

$$= (V_{max})_{inverter} / V_{oc(-1^\circ)} = 1100 / 53.26 \approx 20$$

And the minimum number of modules per string is:

$$= (V_{mp, min})_{inverter} / V_{mp(+60^\circ)} = 600 / 36.87 \approx 16$$

Hence, it is convenient to choose 18 modules in series per one string.

Now to find out the number of strings to be connected in parallel as follows:

$$= 2 \times 1000\text{kW} / (18 \times 540) = \underline{208}$$

Hence, PV array is configured as shown in Figure (21) and consists of 208 parallel strings, each formed of 18 modules connected in series. As seen in the Figure, the parallel strings are subdivided into 16 subarrays for ease of circuitry connections and protection. Each subarray consists of 13 strings. Hence, the total number of modules is = 18 x (13 x 16) = 3744 modules.

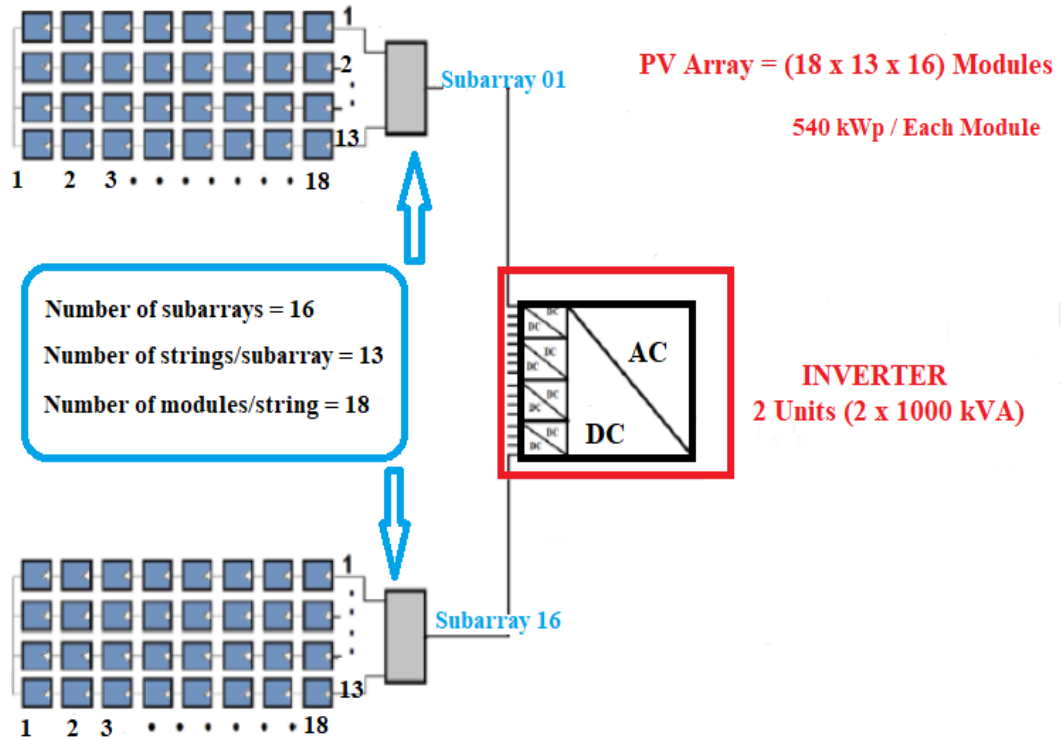


Figure 21. Two MW PV system layout

4-1-3 Comparison Between the Two Methods

It is worthwhile to compare herein the benchmarked system layout obtained from PVSYS software with the system layout obtained from applying the design equations. Table (12) shows this comparison.

Table 12. Comparison between system layout from the two methods

Design layout from PVSYS		Layout from Design Equations	
PV module		PV module	
Manufacturer	Generic	Manufacturer	SunPower
Unit nom. Power	440 Wp	Unit nom. Power	540 Wp
Number of modules	4545	Number of modules	3744
Nominal (STC)	2000 kWp	Nominal (STC)	2000 kWp
Modules	1515 x 3 in series	Modules	208 x 18 in series
P mpp @50°C	1838 kWp	P mpp @50°C	1900 kWp
U mpp @50°C	504 V	U mpp @50°C	41 V
I mpp @50°C	3648 A	I mpp @50°C	3420 A

Inverter		Inverter	
Manufacturer	Generic	Manufacturer	ABB
Type	Multi-string	Type	Centralized
Unit nom. Power	90 kW ac	Unit nom. Power	950 kW ac
Number of inverters	18	Number of inverters	2
Total power	1620 kW ac	Total power	1900 kW ac
Operating voltage	420-800 V	Operating voltage	600-800 V

The layout obtained from applying the design equation uses better state-of-the-art technological components, and hence gives better system outcomes and configuration.

These results will be adopted in the following simulation process.

4.2. Baghdad Distribution Network

4.2.1. Interconnection between networks

The distribution network in any power grid is interconnected with both transmission and generation networks. Traditionally, the generation voltage level is a low voltage level due to limited insulation capabilities of synchronous generator windings inside the electrical generating stations. The conventional output voltage for generators is ≤ 11 kV, though some newly utilized generators may have higher output voltage. Therefore, generating stations are equipped with step-up transformers at the connection point with transmission network in order to step-up the voltage to a level suitable for power transmission. The system voltage for transmission in Iraq ranges between 132 kV and 400 kV. This has the configuration of two inter-connected rings, one rated at 132 kV and the other at 400 kV. The inner ring would be the 132 kV while the outer ring is the 400 kV ring. The distribution network on the other hand is conventionally rated at low voltage level to be capable of distributing electrical power to consumers inside the cities. Electrical power demand at the distribution network consists of industrial and residential loads. Therefore, transmission networks are connected to distribution networks through step-down substations in which the voltage level is stepped down. Figure (22) show the 132 kV ring which is supplied from the

400 kV ring at two sides, Baghdad East, and Baghdad West substations. This ring is in turn interconnected with 132/33 kV MV substations.

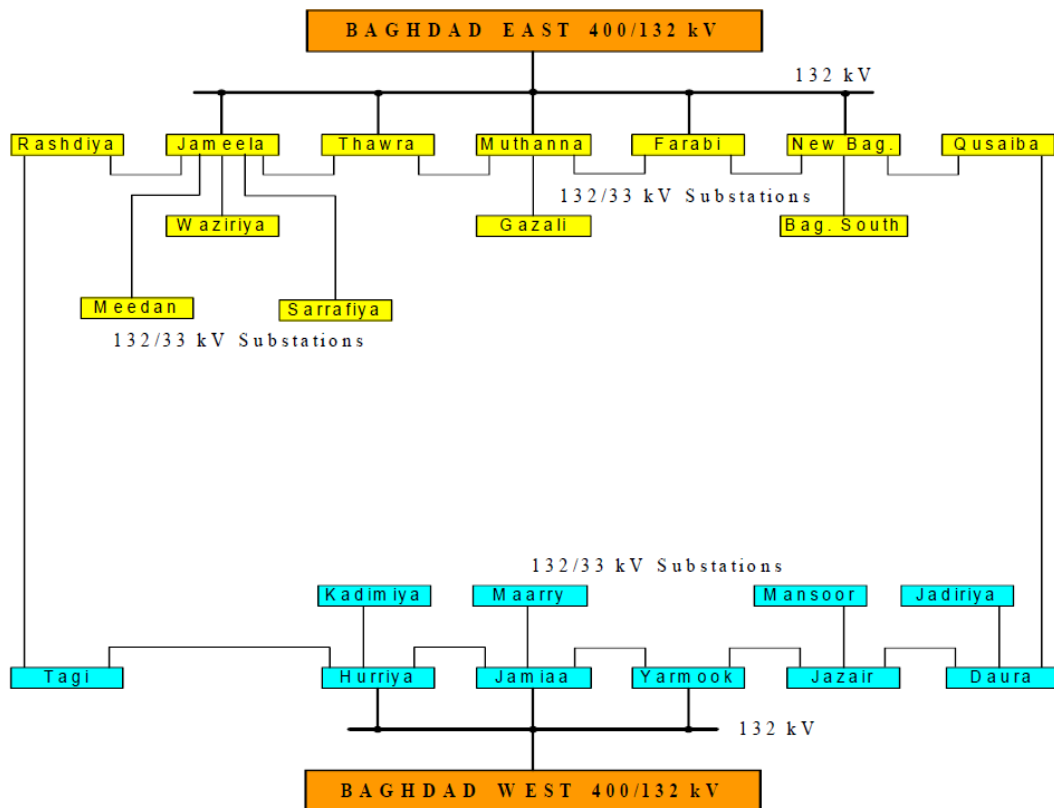


Figure 22. Baghdad city power grid

4.2.2. Baghdad West 33/11 kV substation

The step-down substations in Iraq are rated at 33 kV and 11 kV which are interconnected to ensure availability of electrical power supply to consumers during fault conditions. Each of the 33/11 kV distribution substations is supplied from two 33 kV feeders to ensure better continuity of supply to consumers in case of fault conditions. Baghdad West substation taken as a case study in this research is supplied from 33 kV feeders as shown in Figure (23).

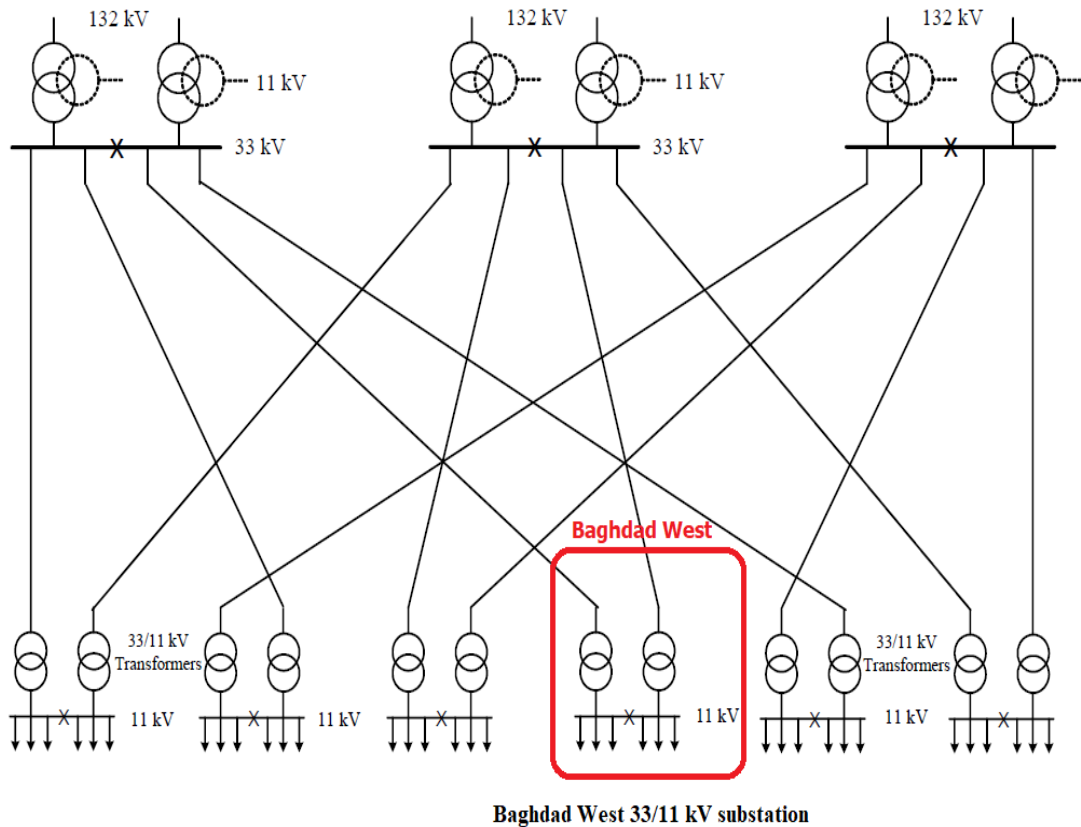


Figure 23. Baghdad city 33/11 kV distribution network

4.2.3. Baghdad West 33/11 kV simulation with ETAP

To carry out simulation of the substation in this case study, the following steps are to be proceeded:

- A. All the data for the substation components are collected from the substation documentary office. This includes the short circuit MVA rating of the main 33 kV bus, the nameplate data for the main two 33/11 kV transformers, the main busbar, all outgoing cables and feeders, utility transformer and local loads, and outgoing load at each output feeder.
- B. The single line diagram of the substation is drawn in ETAP environment as built in its actual state in the grid. The system circuit is shown in Figure (24).
- C. The collected data for all network components is given as input data to the program and written into the software library.

D. Running the load flow calculation for the system which implemented using Newton-Raphson Method of iterative solution to the system equations. The calculation is carried out according to three steps as shown in the next section.

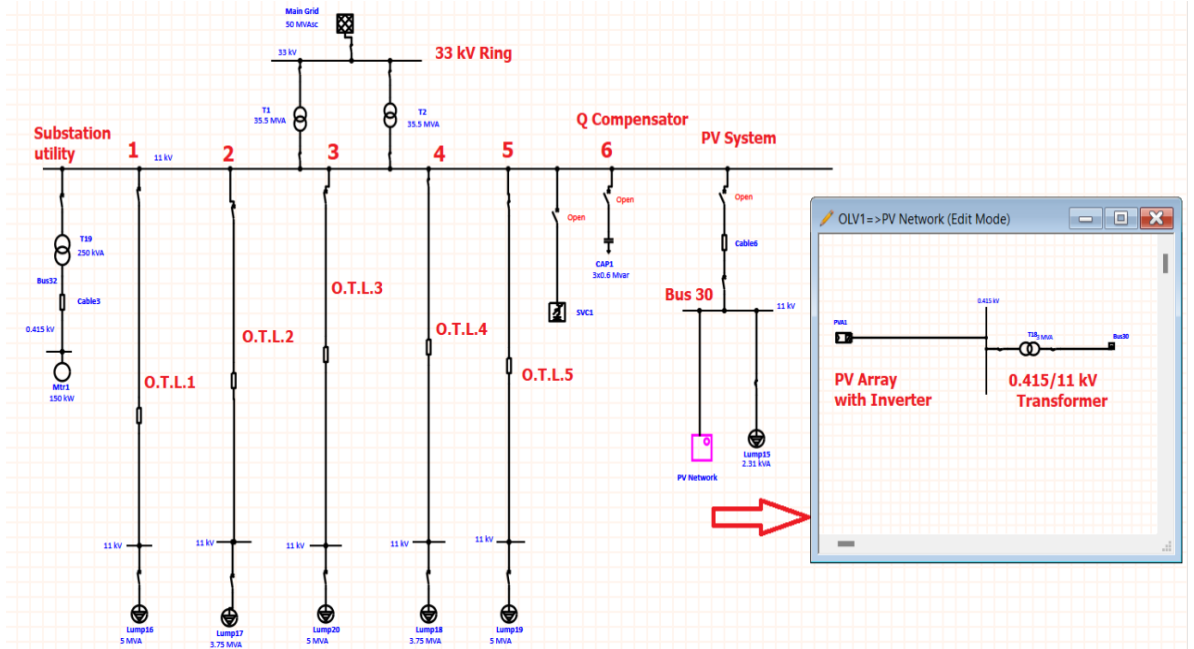


Figure 24. SLD of Baghdad West Substation Network (in ETAP Environment)

The details of the substation component's ratings are as given in Appendix D.

4.3. Power Flow Case Studies

As seen in section 5-1, the network SLD was drawn on ETAP environment and prepared for load flow calculations. It is noted from the network diagram that every distribution substation is equipped with a capacitor bank, suitably rated, and connected to the outgoing busbar for reactive power compensation. This is achieved by delivering capacitive VAR to the grid to compensate for the inductive VAR caused by motor loads. Thus, it improves the voltage drop at load buses and improves the power factor on the grid. The SVC is rated at 20 MVAR and connected at the 11kV bus.

Power flow calculations are carried out using ETAP environment through three various campaigns. It is firstly required to check out the system status by carrying out the calculation without PV units and without connecting the SVC. Secondly, the load flow is calculated by allowing for the SVC to interfere but keeping the PV units out of

the system. The third campaign is achieved when the system performance is brought to improvement by the addition of the proposed 2 MVA solar PV system. These cases are discussed separately in the following subsections.

4.3.1. Case 1: without PV, without SVC

Table 13. Study case 1, general results

Study Case 1	Without PV, without SVC
Buses	9
Branches	9
Power Grids	1
Loads	6
Load-MW	39.177
Load-MVAR	27.391
Generation-MW	1.359
Generation-MVAR	3.984
Loss-MW	0.0002
Loss-MVAR	0.0002

Table 14. Study case 1, main grid results

ID	Rating/Limit	Rated kV	MW	MVAR	Amp	% PF
Main Grid	50 MVA	33	39.177	27.391	836.3	81.96 (*)

(*) The power factor at the main grid is below accepted level ($\geq 85\%$).

Table 15. Study case 1, load flow results at busbars

Bus ID	Nominal kV	%Voltage	MW Load	MVAR Load	Amp Loading
Bus1	100	100	39.177	27.391	836.3
Bus2	100.2	99.83	39.097	24.673	2431
Bus25	98.16	95.68	8.356	5.179	539.3
Bus26	98.68	96.74	6.293	3.9	401.7

Bus28	98.68	96.74	6.293	3.9	401.7
Bus29	98.16	95.68	8.356	5.179	539.3
Bus31	98.16	95.68	8.356	5.179	539.3
Bus32	99.73	100.01	0.162	0.0703	245.7
Bus33	99.44	99.72	0.162	0.0703	246

Table 16. Study case 1, load flow results at loads

ID	kW	kVAR	Amp	% Loading	% V Terminal
Lump16	8356.4	5178.8	539.3	102.7 (*)	95.68
Lump17	6293.3	3900.2	401.7	102	96.74
Lump18	6293.3	3900.2	401.7	102	96.74
Lump19	8356.4	5178.8	539.3	102.7	95.68
Lump20	8356.4	5178.8	539.3	102.7	95.68
Mtr1	161.7	70.3	246	100.3	99.72

(*) Load buses are all overloaded.

Evaluation of Case-1 results:

- A. The voltage level at all busbars is within the standard range of drop limit which is not to exceed $\pm 5\%$, but some buses show marginal voltage drop and should be monitored which are buses 26, 28, 29, and 31 in Table (15).
- B. The power factor at the main grid is (81.96%), which is below accepted level ($\geq 85\%$).
- C. The percentage loading at all loads in Table (16) exceeds the full load limit which should be below full load level for safe operation.

D. The voltage level at all load busbars in Table (16) is within the standard range of drop limit which is not to exceed $\pm 5\%$, but all, except motor load bus, show marginal voltage drop and should be monitored.

4.3.2. Case 2: Effect of SVC on grid performance

In this case, the effect of SVC rating on the performance of the main grid is studied. For this purpose, three values for SVC rating are selected to examine the system performance at each rating and compare the results. These ratings are 1800kvar, 6000kvar, and 9000kvar. The performance parameters are the power factor (P.F.), the main grid current (Amp.) in per unit, and the reactive power supplied by the grid (Source Mvar) in per unit. The comparison results are shown in Table (17).

Table 17. Study case 2, SVC effects on grid performance

SVC	1800 kvar	6000 kvar	9000 kvar
P.F.	0.8378	0.8807	0.9086
Amp. (P.U.)	0.816	0.778	0.753
Source Mvar (P.U.)	0.509	0.421	0.359

Better performance is obtained with a higher rating of SVC as in such case the current and reactive power supplied by the grid are lower whereas a higher power factor is recorded. These effects are presented in Figure (25). Hence, the rating selected for SVC in the next steps of this study is 9000kvar.

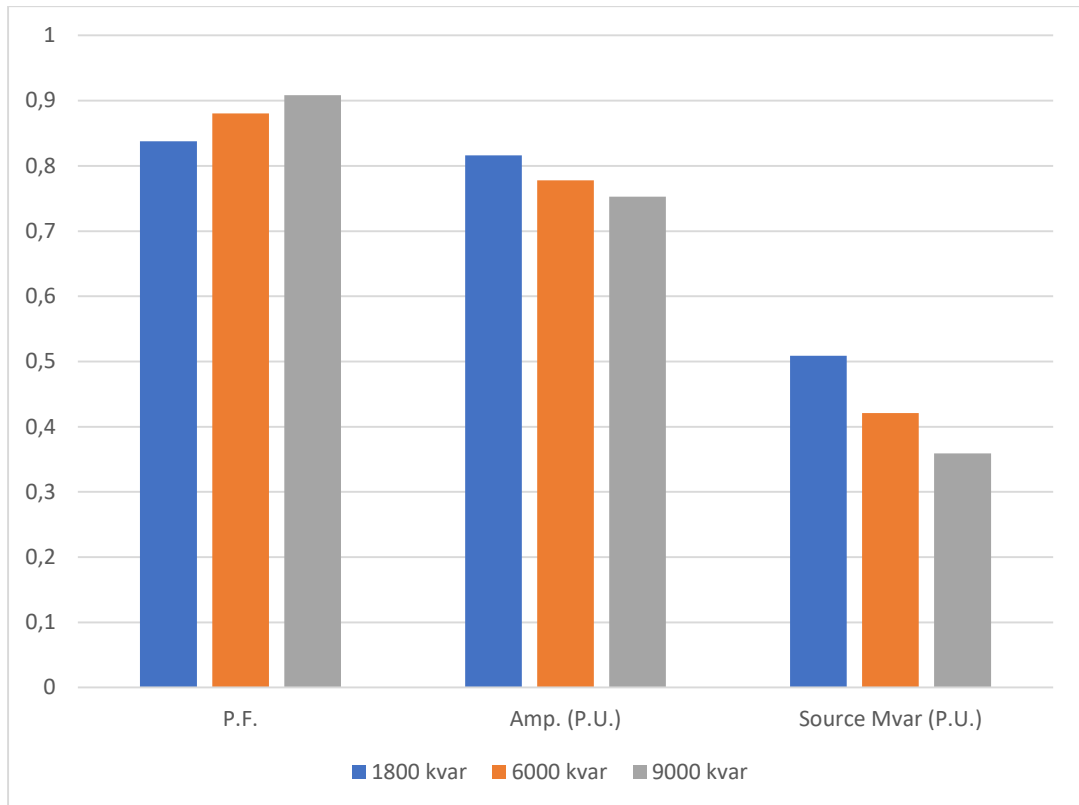


Figure 25. SVC rating effects on grid performance

4.3.3. Case 3: without PV, with SVC (rating = 9000kvar)

Table 18. Study case 3, general results

Study Case 3	Without PV, with SVC
Buses	9
Branches	9
Power Grids	1
Loads	6
Load-MW	37.789
Load-MVAR	14.453
Generation-MW	39.139

Generation-MVAR	17.986
Loss-MW	1.349
Loss-MVAR	3.533

Table 19. Study case 3, main grid results

ID	Rating/Limit	Rated kV	MW	MVAR	Amp	% PF
Main Grid	50 MVA	33	39.139	17.986	753.6	90.86

Table 20. Study case 3, load flow results at busbars

Bus ID	Nominal kV	%Voltage	MW Load	MVAR Load	Amp Loading
Bus1	33	100	39.139	17.986	753.6
Bus2	11	99.65	39.072	24.659	2434
Bus25	11	95.49	8.35	5.175	540
Bus26	11	96.55	6.289	3.897	402.2
Bus28	11	96.55	6.289	3.897	402.2
Bus29	11	95.49	8.35	5.175	540
Bus31	11	95.49	8.35	5.175	540
Bus32	0.415	99.81	0.162	0.0703	246.2
Bus33	0.415	99.53	0.162	0.0703	246.5

Table 21. Study case 3, load flow results at loads

ID	Rating/Limit	kW	kVAR	Amp. (A)	%P.F.	% Loading
CAP1	-9000 kVAR	0	-8936.7	470.7	0	99.6
Lump16	10000 kVA	8350.2	5175	540	85	102.9
Lump17	7500 kVA	6288.6	3897.3	402.2	85	102.2
Lump18	7500 kVA	6288.6	3897.3	402.2	85	102.2
Lump19	10000 kVA	8350.2	5175	540	85	102.9
Lump20	10000 kVA	8350.2	5175	540	85	102.9
Mtr1	150 kW	161.7	70.3	246.5	91.71	100.5

(*) Load buses are all overloaded.

Evaluation of Case-3 results:

- A. The voltage level at all busbars is within the standard range of drop limit which is not to exceed $\pm 5\%$, but still some buses show marginal voltage and should be monitored which are buses 26, 28, 29, and 31 in Table (20).
- B. The power factor at the main grid is now corrected to be (90.86%) which is higher than the accepted level ($\geq 85\%$).
- C. The percentage loading at all loads in Table (21) is still exceeding the full load limit which should be below full load level for safe operation.
- D. Loading on all cables and transmission lines is acceptable, and voltage drop margin as well.

4.3.4. Case 4: with PV, with SVC (rating = 9000kvar)

Table 22. Study case 4, general results

Study Case 4	With PV, with SVC
Buses	11
Branches	11
Power Grids	1

Loads	7
Load-MW	37.792
Load-MVAR	14.454
Generation-MW	39.148
Generation-MVAR	17.901
Loss-MW	1.356
Loss-MVAR	3.447

Table 23. Study case 4, main grid results

ID	Rating/Limit	Rated kV	MW	MVAR	Amp	% PF
Main Grid	50 MVA	33	37.161	17.901	721.7	90.09

Table 24. Study case 4, load flow results at busbars

Bus ID	Nominal kV	%Voltage	MW Load	MVAR Load	Amp Loading
Bus1	33	100	37.161	17.901	721.7
Bus2	11	99.65	39.073	24.763	2436
Bus25	11	95.5	8.35	5.175	539.9
Bus26	11	96.56	6.289	3.897	402.2
Bus27	0.415	100.12	1.986	0	2760
Bus28	11	96.56	6.289	3.897	402.2

Bus29	11	95.5	8.35	5.175	539.9
Bus30	11	99.74	1.976	0.103	104.1
Bus31	11	95.5	8.35	5.175	539.9
Bus32	0.415	99.82	0.162	0.0703	246.1
Bus33	0.415	99.53	0.162	0.0703	246.5

Table 25. Study case 4, load flow results at loads

ID	kW	kVAR	Amp. (A)	%P.F.	% Loading
CAP1	0	-8937.8	470.7	0	99.7
Lump15	1.84	1.38	0.121	80	99.7
Lump16	8350.4	5175.1	539.9	85	102.9
Lump17	6288.8	3897.4	402.2	85	102.2
Lump18	6288.8	3897.4	402.2	85	102.2
Lump19	8350.4	5175.1	539.9	85	102.9
Lump20	8350.4	5175.1	539.9	85	102.9
Mtr1	161.7	70.3	246.5	91.71	100.5

(*) Load buses are all overloaded.

Evaluation of Case-4 results:

- A. The voltage level at all busbars is within the standard range of drop limit which is not to exceed $\pm 5\%$, but still some buses show marginal voltage and should be monitored which are buses 25, 26, 28, 29, and 31 in Table (24).
- B. The power factor at the main grid is still corrected to be (90.09%) which is higher than the accepted level ($\geq 85\%$).

- C. The percentage loading at all loads in Table (25) is still exceeding the full load limit or approaching it which should be below full load level for safe operation.
- D. Loading on all cables and T.L.s is acceptable, and voltage drop margin as well.

Comparing the results of cases 3 & 4 shows the conclusion that provision of PV units has limited effects on load bus voltages and load bus loadings as shown by comparing results in Tables (18) to (25). However, we can notice a remarkable improvement in the grid supplied power and ampacity as shown in Table (26) and Figure (26).

Table 26. Comparison between results of cases 3 and 4

CASE	MW	MVAR	Amp	% PF
3	39.139	17.986	753.6	90.86
4	37.161	17.901	721.7	90.09

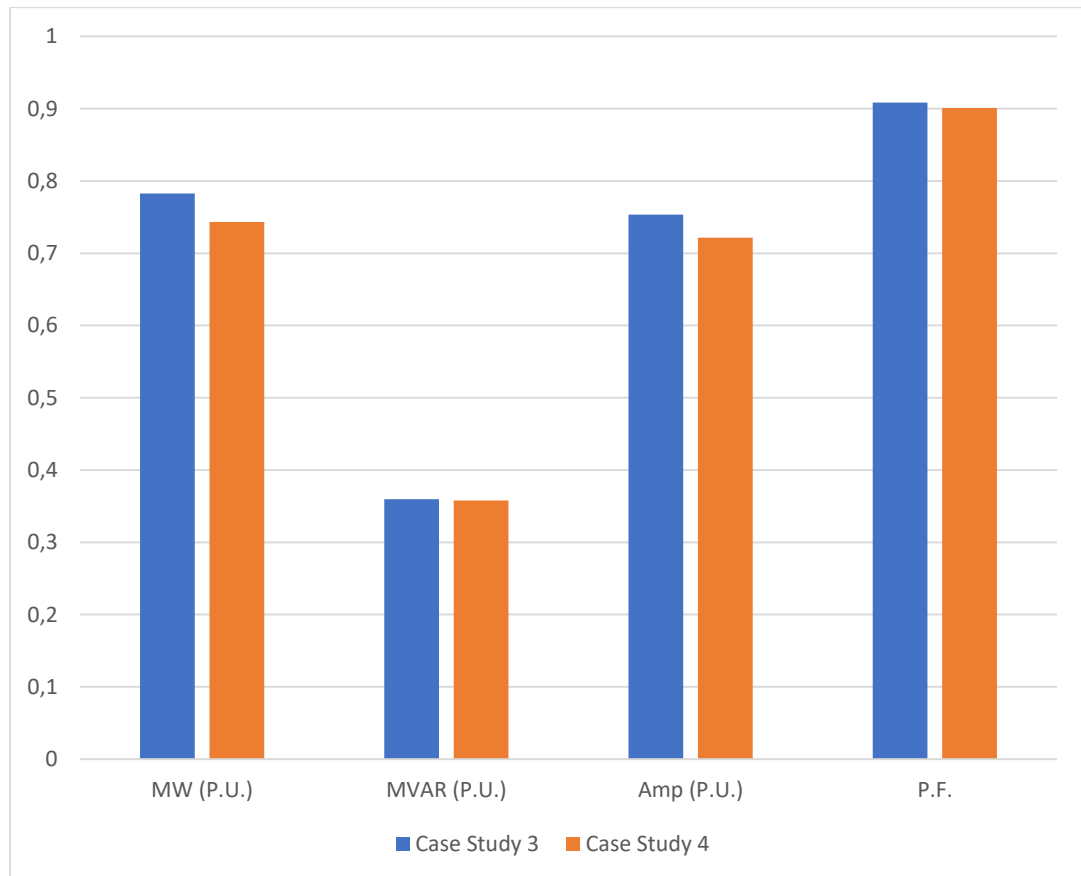


Figure 26. Improvements offered by addition of PV units (case 4)

4.4. Harmonic Analysis

4.4.1. Harmonic Causes and Effects

Fundamentals of harmonics fall under the power quality analysis concept. To go over the definition of harmonics; the presence of harmonics in electrical systems means that current and voltage are distorted and deviate from sinusoidal wave forms. They are represented by waves having a frequency that is an integral multiple of the fundamental frequency. Harmonic currents are caused by nonlinear loads mainly connected to power system. The harmonics overlay themselves on the fundamental waveform, distorting it and changing its magnitude. So, for high current mainly it will increase the current losses in transformers and generators. It will also increase current, hence, resistance losses in conductors, transformers, and generator winding. It could also overload neutrals. Now let us look at why high background voltage distortion or the total harmonic distortion (THD) voltage causes problems. First, it could cause failures of switch mode power supplies on PLC's, computers, and instruments. So, if any of these problems exist, then after some time it could be attributed voltage harmonic distortion problems. Therefore it is essential to perform a harmonic study for power system to verify its operating conditions, e.g., if a generator is out of voltage regulator, it could malfunction if there are serious voltage distortions in the system. It can also cause false reading on critical sensors and instrumentation, increased operating temperature on induction motor winding and rotor bars leading to premature motor failures. A nonlinear load is one that draws current in a non-sinusoidal fashion even when the voltage is a perfect sine wave because of the chopping that happens in power electronics. These loads typically include static power converters, pulse with modulated drives or switch mode power supplies very similar to DC Power electronics inverters which are very common now with solar PV. Some of the renewable inverters are being installed for solar farms, arc furnaces for heavy industry variable speed drives which are found in offshore platforms as well as in most industrial sites and even fluorescent lights.

4.4.2. International Standards on Harmonics

It is essential to distinguish between the IEEE 519 standard issued in 1992 and its 2014 revision as a starting point in essence of a guideline to be used by engineers for power system design consideration and acceptable harmonic content limits for individual equipment to be obtained from manufacturer. The IEEE 519 standard concerns the harmonic distortion introduced into the grid at the point of common coupling (PCC). So, if the concern is on harmonic contents within the site, then certainly we can use the IEEE 519 standard limits. However, it is customary to find the scope of work is to examine how to apply it on the individual equipment harmonic limits, it is a good idea to always start with the manufacturer. The differences between the two standard versions, as shown in Figure (27), start with the limits for total

demand

distortion.

**New limits (for V = Less than 1 kV):
5% for individual distortion and 8% for THD**

Table 1 in Standard IEEE 519 (2014)			Table 10-2 in Standard IEEE 519 (.1992)			
Bus voltage at PCC	Individual harmonic (%)	THD (%)	THD	Special Application	General Application	Dedicated System
$V \leq 1.0 \text{ kV}$	5	8	THD	3%	5%	10%
$1 \text{ kV} \leq V \leq 69 \text{ kV}$	3	5				

Figure 27. IEEE 519 (1992) vs IEEE 519 (2014)

Examining these tables shows that the total demand distortion column on the right-hand side represents short circuit ratio (SCR), which is the maximum short circuit current at PCC over the maximum low demand current of fundamental frequency. Again, at PCC on the first column on each one of these tables. Under SCR of 20, say typically 10 expresses a very large load. An SCR that is greater than 1000 for example, typically represents very small loads or in other words a weak power source. A utility that is very weak with a large demand current relative to the rated current will show greater waveform distortion. On the other hand, a very stiff power source or large short-circuit contribution operating at a low demand current will show a decreased waveform distortion. Continuing with some of the significant changes between 1992 and 2014 standard is the following. On the right-hand side of table 10-2 of 1992 version, the voltage ranges from 120 volts to 69 kV which called for a THD voltage of 3% for special applications and 5% for general systems with 10% allowed for dedicated systems. Over on the left-hand side, for table number one we now have a special bus voltage range that has been added. So now we have a new limit for buses under one kV. The individual is 5% and the total harmonic distortion is 8%. So that's a significant change and for bus voltages above 1.0 kV and up to 69 kV. The total harmonic distortion (THD) voltages remain the same individual is at 3% and the THD is 5%. So that didn't really change. So, the main impact you would have had if your facility or the mainly commercial buildings for example, had an income at the PCC that is under one kV. You now have an increase allowable THD voltage which increased from 3% to 5%. Here's just another representation of voltage distortion limits. This has now been built into the new version of its tab.

4.4.3. Harmonic Analysis by ETAP

On ETAP environment one can find a harmonics rule book that contains the limits for harmonic voltages that could be applied not just at the PCC, but if the user likes to have different global settings or specifically at individual locations. IEC 61000-3-6 has also been updated. The new tab harmonics rulebook and we'll go over that here in a, in a brief example, before we go over harmonic sources and software modelling, where the new rule book is found.

Running harmonic analysis mode on ETAP with the new version of its application complies with the new IEEE 519 (2014). The new rule book allows to customize proceeding with the following preparation steps:

1. Pull down menu, go over to harmonics as you can have multiple limits based on the harmonic standard that you will be applying (e.g., the P 5 1920 14, which is used in north America, or the British Standard G 54-1, or the IEC 61000-3-6 (2008), which is typically used in Europe).
2. The current harmonic limits for a particular location in the network are performed with a local compliance rule selected from the rule book considering short circuit current.
3. SCR will have an impact on waveform distortion. So, either select, calculate, and have allowed the short circuit study engine to perform that or you could specify user defined if you have a recent enough study and you want to use that value.
4. The other item that has been enhanced for 2014 is the transmission line cable model as well as the skin effect model for transformers, synchronous motors, induction machines. For transmission line model, you now can use the short line model as well as a long line model. Uh and you get to specify when the long line model or cable begins.
5. For inverters, under the reference put the data sheet is going to be a current source, then once it is created go to edit first starting from the top and then work down to the bottom. The fundamental frequency is going to be 50 hertz. This is going to be a six pulse. So, you have your 5th 7th, 11th 13th and so on. The fundamental current magnitude in amps is specified according to the results from load flow analysis.
6. The next step is to switch over to the harmonic analysis mode from the toolbar. This will allow you to select which buses you want to display on the results for the plots and as well as what you want reported on the one-line diagram.
7. Try to focus on specified locations: main bus, which is the PCC, bus number X₁ and bus number X₂, which is on the line side of the inverter.
8. Select okay and then run a harmonic analysis and the first thing that you see on the screen is the THD at each of the buses that have been selected.
9. The harmonic order slider is a very useful tool in the sense that as it is scrolled to the right, the harmonic order is being selected.
10. Check and print the report, and display on the right-hand side, the harmonic analysis view by displaying the harmonic order slider.

4.4.4. Case Study: Harmonic Analysis using ETAP

The harmonic analysis settings are firstly pre-set for each item in the single line diagram of the substation under study. The following assumptions are made:

1. The PV inverter harmonic setting is specified as a current source with six pulse converters.
2. The loads attached to the receiving end of the substation are linear.

Accordingly, the harmonic analysis is performed conducting two scenarios concerning the main distribution transformers harmonic contribution as follows:

- A. The distribution transformers have considerable magnetizing current effect; thus, they contribute to the THD on the main grid.
- B. The distribution transformers are of negligible magnetizing current effect; thus, they do not contribute to the THD on the main grid.

The results in both cases are taken either viewed on the SLD with Toolbar Viewer or exported as Excel and pdf files.

Case A results:

If the results are presented first by THD viewer, the following Figures (28) to (32) show the harmonic effects resulted taken by individual components.

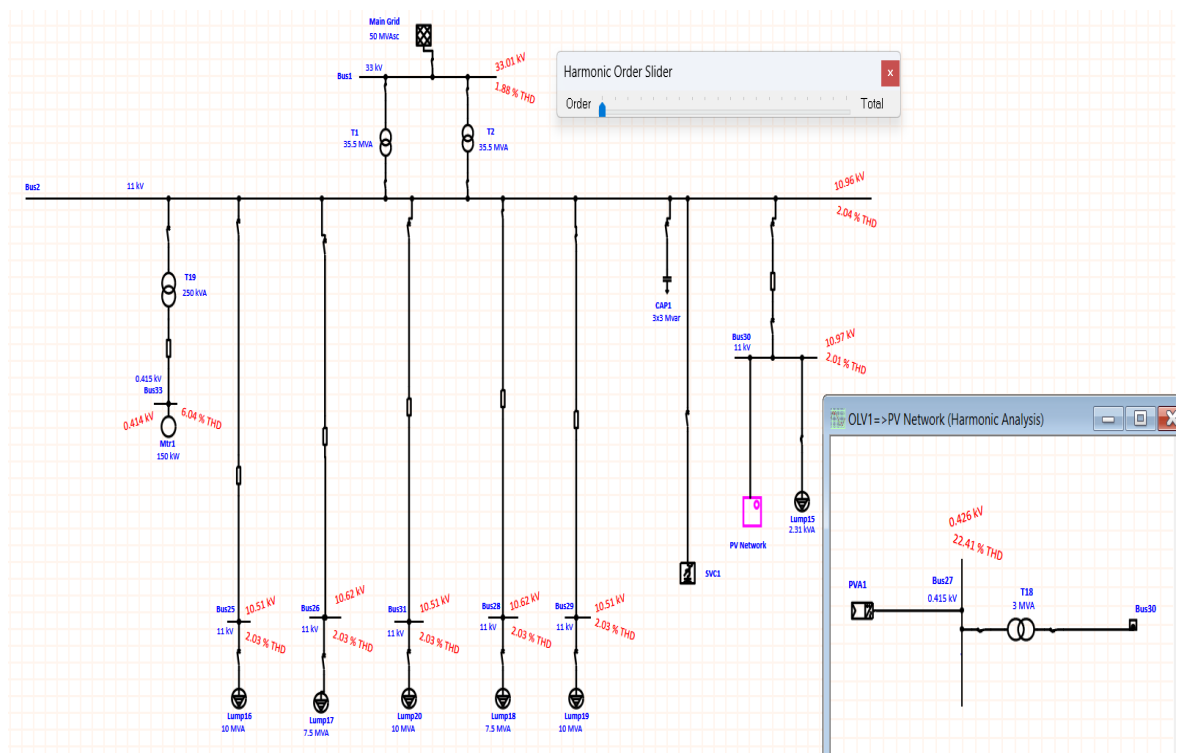


Figure 28. THD viewed on the SLD of the substation.

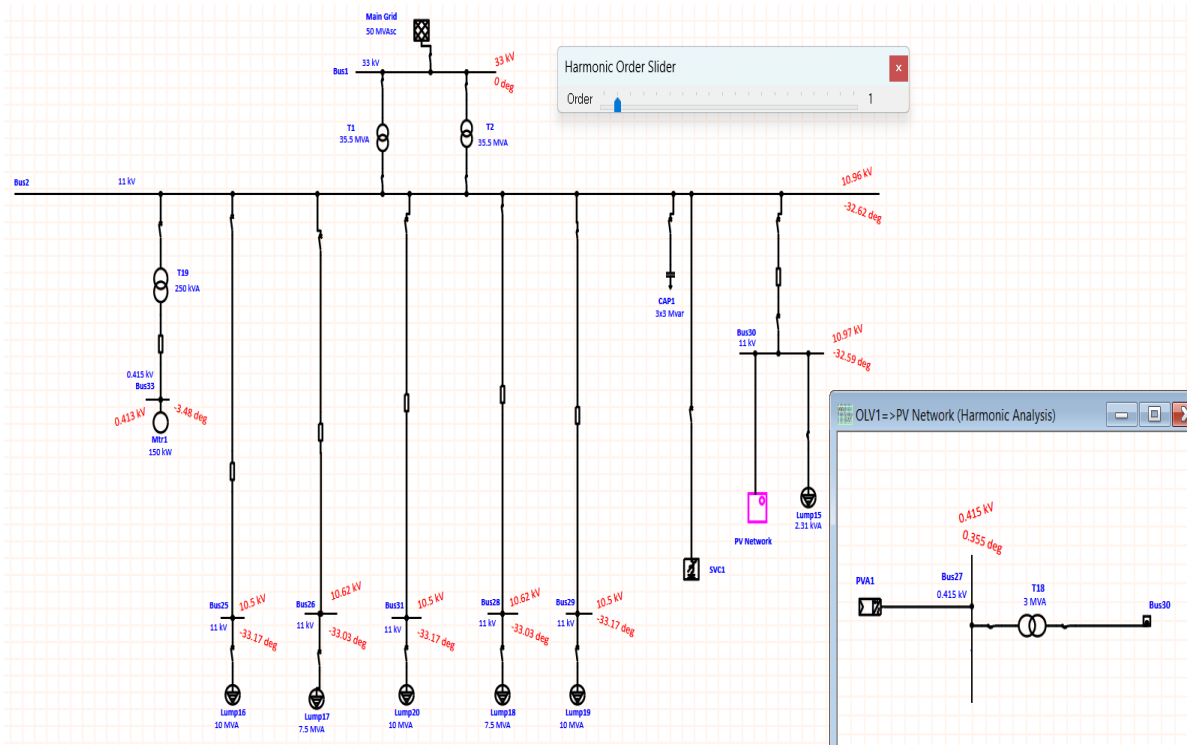


Figure 29. Fundamental components viewed on the SLD of the substation.

Figure (28) shows the THD as viewed on the various buses of the system whereas Figure (29) shows the fundamental components of the harmonic spectrum as viewed on the various buses of the system.

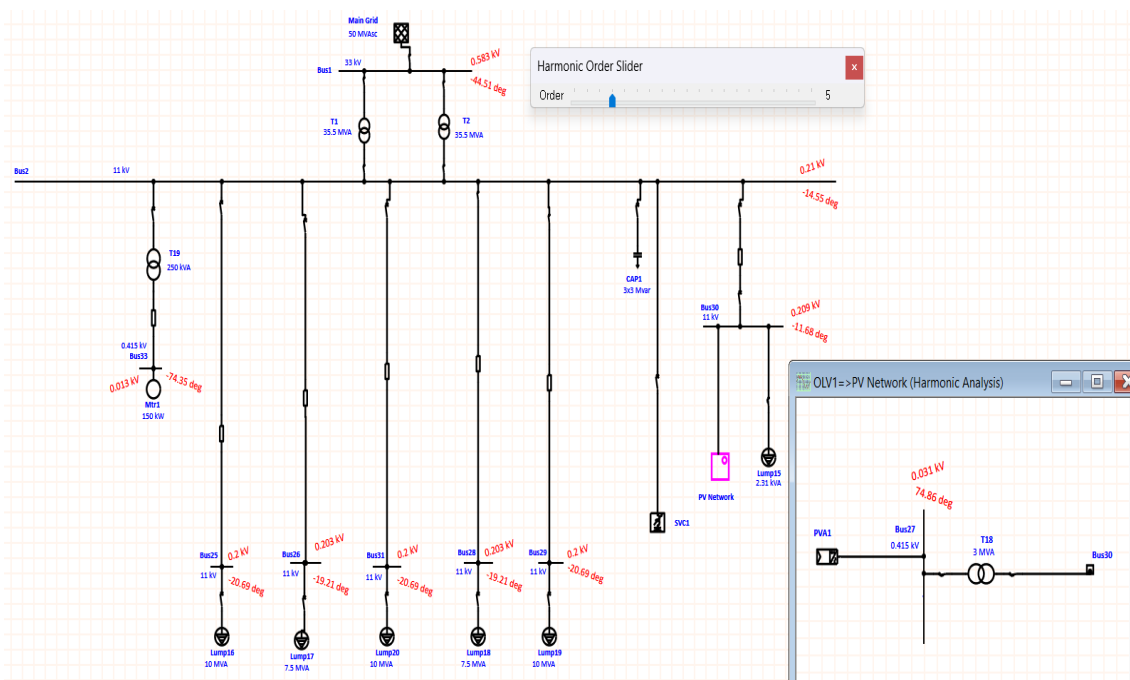


Figure 30. 5th harmonic components viewed on the SLD of the substation.

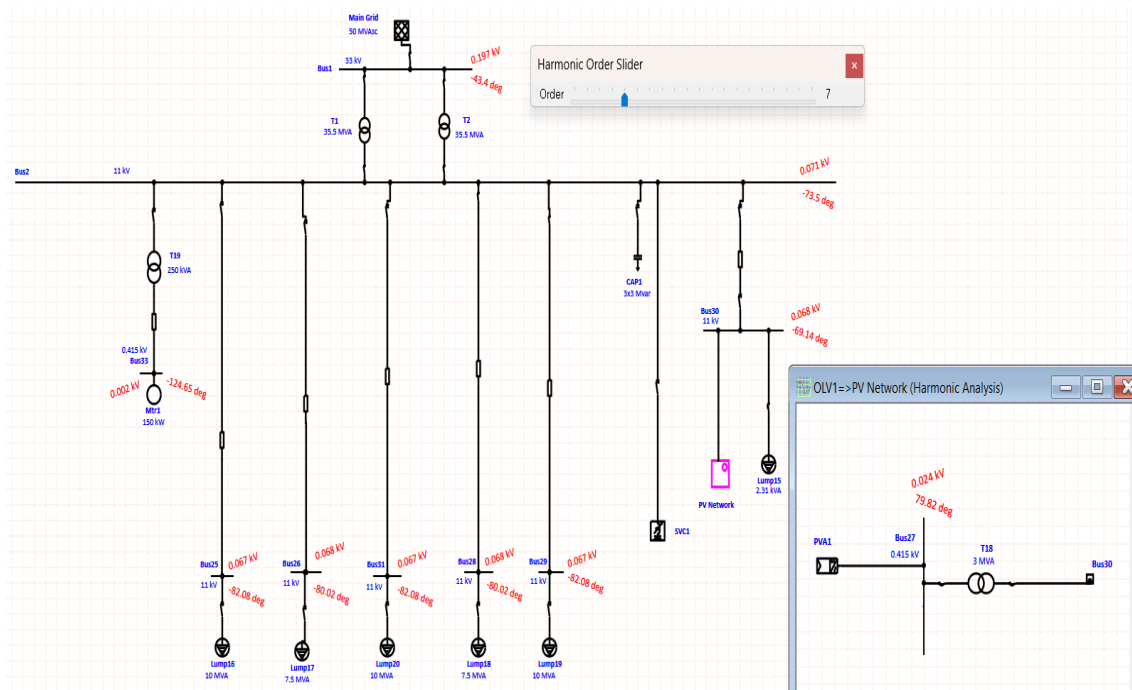


Figure 31. 7th harmonic components viewed on the SLD of the substation.

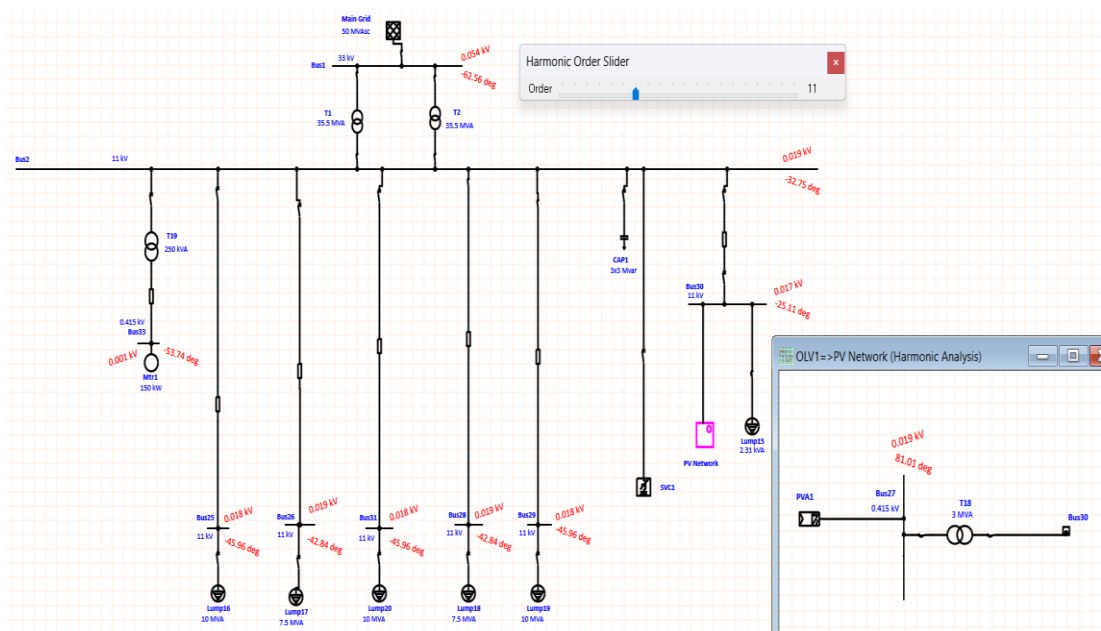


Figure 32. 11th harmonic components viewed on the SLD of the substation.

Figure (30) shows the 5th harmonic components as viewed on the various buses of the system, Figure (31) shows the 7th components and Figure (32) shows the 11th components of the harmonic of the harmonic spectrum as viewed on the various buses of the system.

From Excel files outcome from the analysis, we can tabulate the results in tables showing the harmonic spectrum at the system busbars, and plot bar charts for the harmonic spectrum resulted.

Table 27. Harmonic voltages at system busbar versus frequency spectrum (case A)

Frequency (Hz)	BUS 1 V-Spectrum (%)	BUS 2 V-Spectrum (%)	BUS 25 V-Spectrum (%)	BUS 26 V-Spectrum (%)	BUS 28 V-Spectrum (%)	BUS 29 V-Spectrum (%)	BUS 30 V-Spectrum (%)	BUS 31 V-Spectrum (%)
250	1.76704	1.91124	1.82220	1.84562	1.84562	1.82220	1.89678	1.82220
350	0.59588	0.64451	0.61082	0.62018	0.62018	0.61082	0.61811	0.61082
550	0.16361	0.17697	0.16502	0.16866	0.16866	0.16502	0.15149	0.16502
650	0.11654	0.12606	0.11636	0.11942	0.11942	0.11636	0.09942	0.11636
850	0.06696	0.07242	0.06527	0.06763	0.06763	0.06527	0.04521	0.06527
950	0.05299	0.05732	0.05097	0.05309	0.05309	0.05097	0.03035	0.05097
1150	0.03520	0.03808	0.03286	0.03462	0.03462	0.03286	0.01275	0.03286
1250	0.02934	0.03174	0.02695	0.02857	0.02857	0.02695	0.00844	0.02695
1450	0.02106	0.02279	0.01870	0.02007	0.02007	0.01870	0.00799	0.01870
1550	0.01809	0.01956	0.01577	0.01703	0.01703	0.01577	0.00956	0.01577
1750	0.01360	0.01472	0.01144	0.01250	0.01250	0.01144	0.01244	0.01144
1850	0.01190	0.01287	0.00981	0.0108	0.0108	0.00981	0.01351	0.00981

These voltage spectrums could be plotted as shown in Figures (33) and (34) to examine the harmonic analysis results.

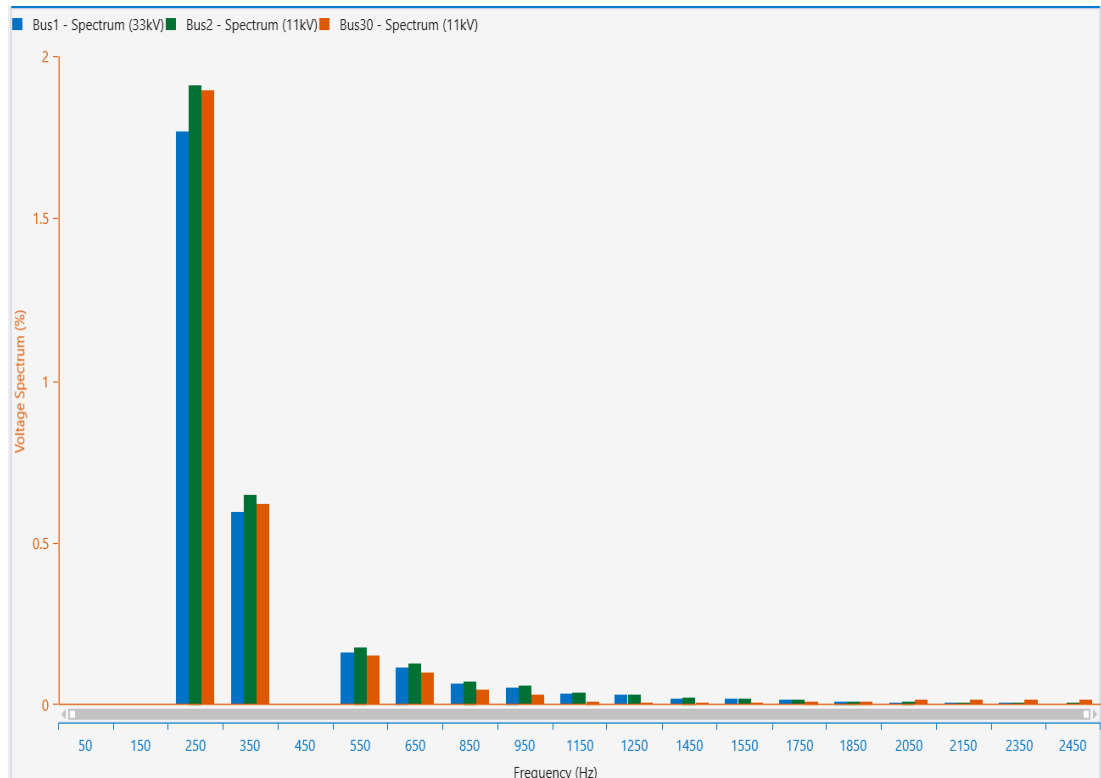


Figure 33. Percentage harmonic voltages at buses 1, 2, and 30 (case A).

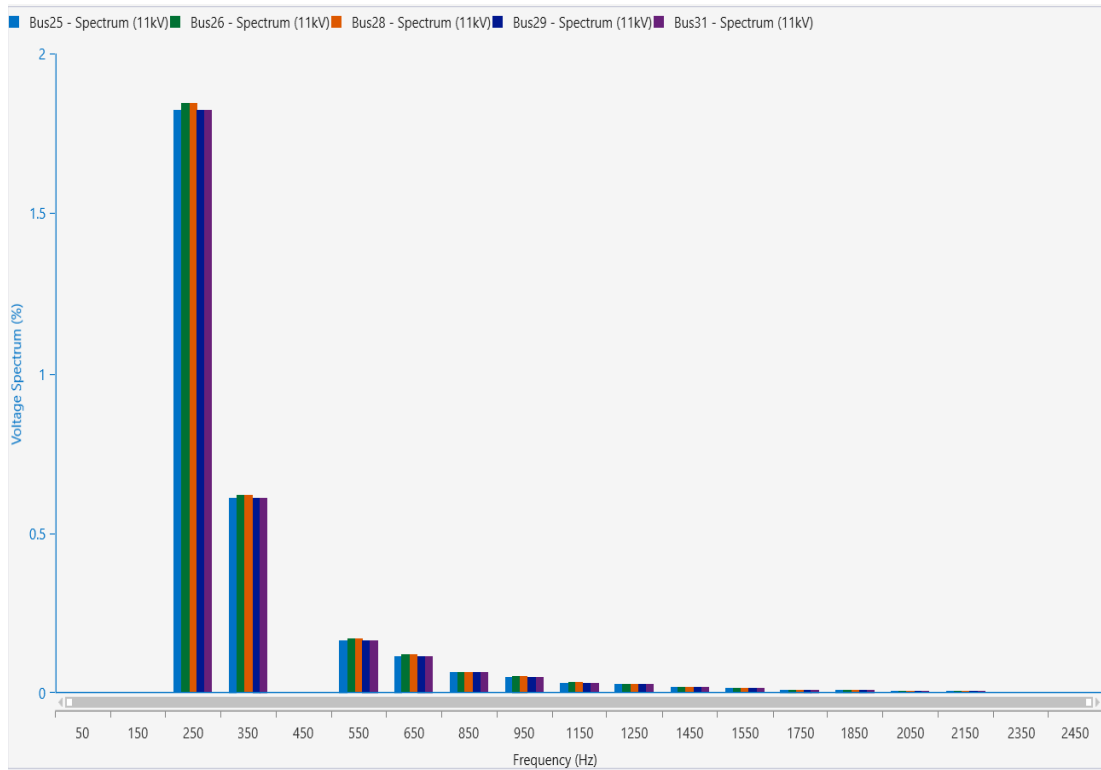


Figure 34. Percentage harmonic voltages at system load buses (case A).

As clearly seen from the results tabulated and plotted above, the harmonic distortion at various locations in the system under study are within the acceptable margin defined by the American standard IEEE 519 (2014) which is 5% for THD for system voltages up to 69 kV. If the obtained results for voltage harmonic distortion is verified, shown in Table (28), then the results for harmonic distortion are as shown.

Table 28. Harmonic voltages at grid busbars (case A)

Harmonic order (h)	Frequency (Hz)	BUS 1 V-Spectrum (%)	BUS 2 V-Spectrum (%)
5	250	1.77	1.91
7	350	0.596	0.645
11	550	0.164	0.177
13	650	0.117	0.126

Case B results:

Considering first the THD at system busbars, the following Figures (35) to (37) which shows bar charts for the THD resulted.

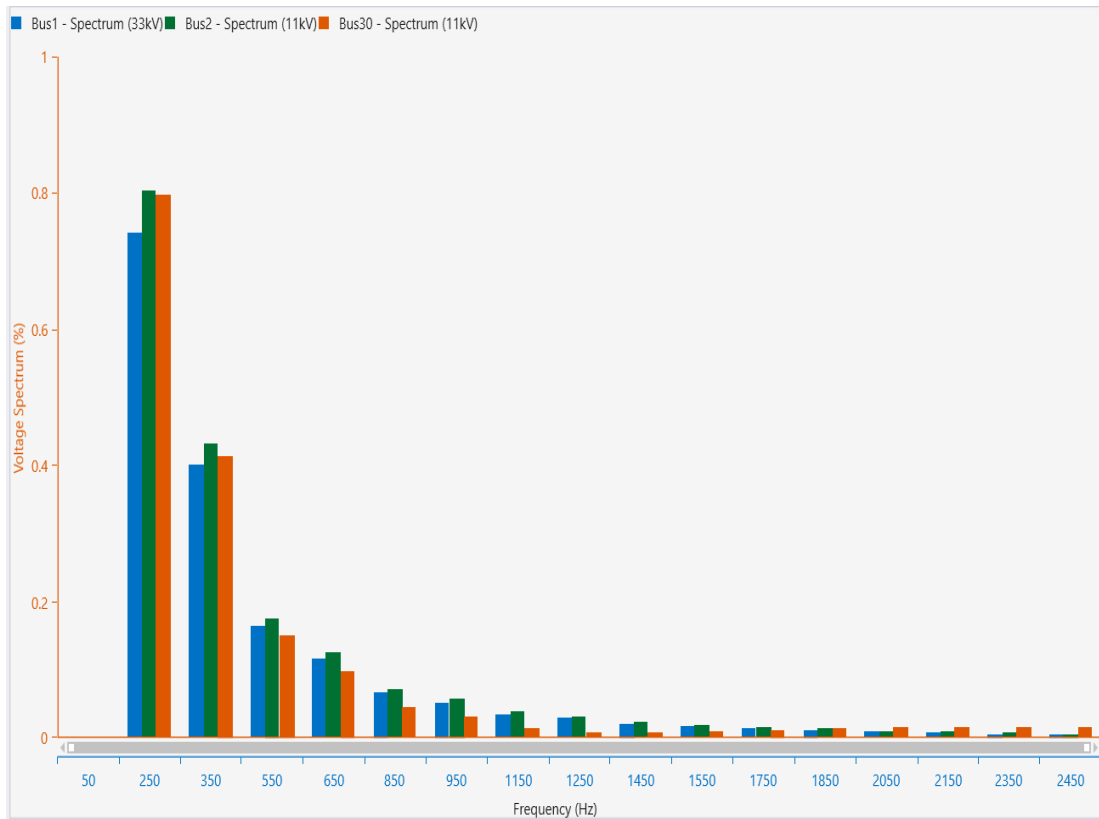


Figure 35. Percentage voltage THD at buses 1, 2, and 30 (Case B).

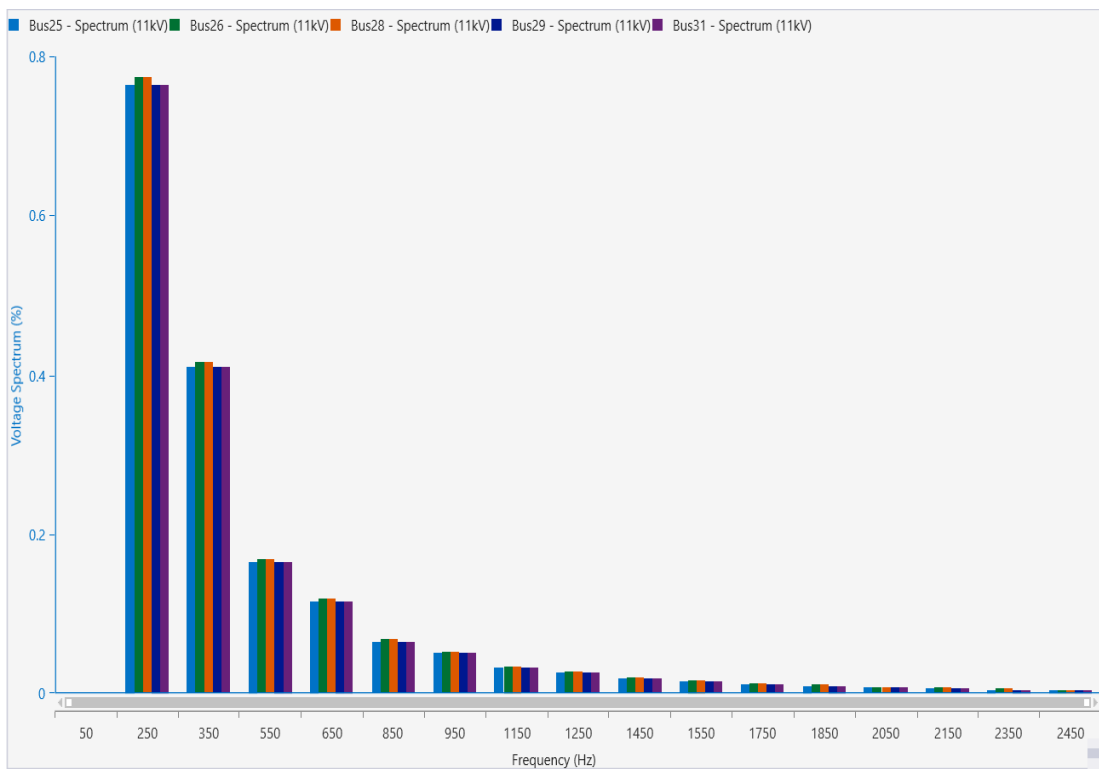


Figure 36. Percentage voltage THD at load buses (Case B).

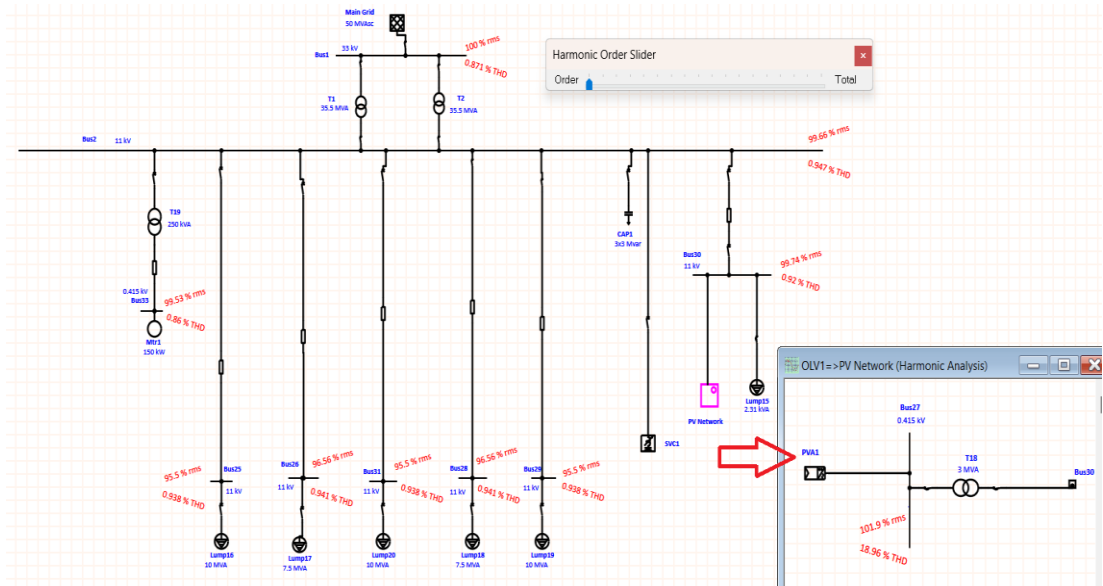


Figure 37. Harmonic Order Viewer put at THD view on SLD of substation (Case B).

It is apparent from Figures (35) to (37), that the THD values at all locations in the system are considerably reduced compared to THD values in case A. This is obviously justified as the no-load magnetizing currents in distribution transformers were neglected.

Now we consider the results outcome in Excel file from the simulation program as shown in Tables (29) and (30).

Table 29. System Harmonics Bus Information (case B)

ID	kV	Fund. (%)	RMS (%)	THD (%)
BUS 1	33.000	100.00	100	0.871
BUS 2	11.000	99.65	99.66	0.974
BUS 25	11.000	95.5	95.5	0.938
BUS 26	11.000	96.56	96.56	0.941
BUS 27	0.415	100.1	101.9	18.96
BUS 28	11.000	96.56	96.56	0.941
BUS 29	11.000	95.5	95.5	0.938
BUS 30	11.000	99.74	99.74	0.92
BUS 31	11.000	95.51	95.5	0.938
BUS 33	0.415	99.53	99.53	0.86

Table 30. Harmonic Voltages as % of Fundamental Voltage (case B)

Harmonic order (h)	Frequency (Hz)	BUS 1 (%)	BUS 2 (%)
5	250	0.741	0.802
7	350	0.4	0.432
11	550	0.164	0.177
13	650	0.117	0.126

The results, as seen in Tables (29) and (30) indicate that significant reduction in individual and total harmonic distortion was found in case B of analysis as compared to case A, although the distortion valued was below the standard limits in both cases. Furthermore, the THD at Bus 27, where the point of common coupling of the PV inverter to the grid is remarked. This six-pulse inverter contributes noticeably to harmonic distortion with a value of 18.96% as seen in Table (29) and 22.41% for case A as seen in Figure 28. Despite this distortion level at Bus 27, the distortion is being mitigated by the star-delta connection (Yd01) of transformer 18 which connects Bus 27 to Bus 30, so that the harmonics at the former busbar are blocked by the zero-sequence circuit and prevented to reach the main bus and load buses. Thus, the distortion at these buses is kept down below the specified limits as shown in Tables (28) and (30).

CHAPTER FIVE

CONCLUSIONS AND RECOMMENDATIONS

5.1. Conclusions

This research has investigated the problem of voltage level deterioration in low voltage distribution networks through a case study on a 11kV substation in Baghdad-West. The study set out to design a Solar PV distributed generation (DG) unit and proposed it as a possible solution to voltage sag problems in distribution systems in addition to enhancing the continuity of supply to consumers. These solar units, as are DC generators in origin, hence are typically interfaced with the grid through PV inverters which function as DC to AC converters. Thus, solar PV units are considered as power resources with adjustable active power (P) and reactive power (Q) power-injections that could enhance the grid voltage level performance. To verify this proposal, the simulation of the distribution substation is conducted using the modern Electrical Transient Analyzer Program (ETAP). The substation data sheets are fed to the program as input data, and the results of the simulation studies are significant in three respects as illustrated below.

1. Solar PV design configuration:

The solar system was designed, as shown in Figure (4-3), such that (18) PV modules were connected in series per one string. Knowing that the module maximum voltage generated is around 41V, this series combination is selected to have string's output voltage which matches the input voltage of the PV inverter (600V-800V). the combinations of strings to be connected in parallel are divided into (16) sub-arrays for ease of construction and feasibility of electrical wiring and protective equipment. Each sub-array contains (13) parallel strings to accumulate currents generated. A central inverter of two units is selected for better reliability and to minimize faults due to unstable operation of multi-units' inverters.

2. Power flow analysis:

Four case studies were examined in this analysis to verify the effect of solar PV units on the voltage level improvement and to determine the optimum SVC ratings for best power factor improvement through static VAR compensation.

For this purpose, the first case study was performed on the system without solar units and without SVC to reveal the importance of both techniques for system performance. Results revealed that though the voltage levels were at marginal drop, the main grid power factor was less than limits defined in standards. In the second case study, the effect of SVC rating on the performance of the main grid is studied. For this purpose, three values for SVC rating are selected to examine the system performance at each rating and compare the results. These ratings were 1800kvar, 6000kvar, and 9000kvar. The performance parameters were the power factor, the main grid current, and the reactive power supplied by the grid. The comparison shows that better performance is obtained with a higher rating of SVC as in such case the current and reactive power supplied by the grid are lower whereas a higher power factor is recorded with SVC rated at 9000kvar.

The third case study was performed without solar PV, but with SVC included. Results showed that the power factor at the main grid is corrected to (90.86%) which is higher than the accepted level ($\geq 85\%$). The loading on all cables and T.L.s are acceptable, and voltage drop margin as well. The effect of reactive VAR compensation on the main grid power factor is clearly verified as expected. In the fourth case, both solar PV and SVC are included. Results showed remarkable improvements in the busbars voltage level which remains within the standard range of drop limit (not to exceed $\pm 5\%$). The power factor at the main grid is still corrected to (90.09%) which is higher than the accepted level ($\geq 85\%$). Comparing the results of cases 3 & 4, although showing limited improvements on load bus voltages by provision of PV units due to limited power ratings of these units, nevertheless, we can notice a remarkable improvement in the grid supplied power and ampacity by about 4.4% as shown in Table (26) and Figure (26).

3. Harmonic analysis:

Sources of harmonics in power grids constitute various types of power electronic-based equipment. PV inverters are considered the major sources due to its intrinsic switching mode of operation while other conventional power elements such as

transformers, cables & transmission lines, and static loads could be considered additional sources. Harmonic analysis is conducted first with all possible harmonic sources taken into account, then the analysis is conducted with PV inverter as the only source that injects harmonic distortion in the grid.

Results for the first case revealed that the harmonic distortion at various locations in the system under study are within the acceptable margin defined by the international standard IEC 61000-3-4. The individual harmonic distortion due to 5th harmonic at bus 1 was 1.77% and at bus 2 was 1.91%, which is below standard limit for this 250 Hz frequency which is 6%. The individual harmonic distortion due to the 7th harmonic at bus 1 was 0.596% and at bus 2 was 0.645%, both are below standard limit for this 350 Hz frequency which is 5%. Individual distortion values due to higher harmonic orders were below standard acceptable limits as well.

Results of the second case show considerable reduction in THD values compared to THD values in the first case as expected due to the ignorance of the contribution of no-load magnetizing currents in distribution transformers T18 & T19, on the total harmonic distortion. THD for buses 1 and 2 were 0.871% and 0.947% respectively. THD at the point of common coupling (Bus 27), where the PV inverter is connected, was 18.96%. This distortion, though higher than permissible limit in the international standard IEC 61000-3-4, it is compensated by the mitigation action offered by the star-delta connection (Yd01) of transformer 18, so that the harmonics from the PV inverter are blocked by the zero-sequence circuit and prevented from reaching the main bus and load buses.

5.2. Recommendations

Further research is recommended to investigate the contribution of PV inverters on THD. This future research should concentrate on the effect of operating switching frequency of inverters on the harmonic distortion. It is required to better understand the relationship between the range of inverter switching frequency and the range of low order harmonic distortion and on higher harmonics as well. Such work would strongly assist the trend of harmonic filters design.

REFERENCES

- Abidin, M. N. Z. (2006). IEC 61000-3-2 Harmonics Standards Overview. *Schaffner EMC Inc., NJ, USA*. Microsoft Word - Harmonics overview 2006 May 06.doc (emcfastpass.com)
- Alfalahi, Saad T. Y., et. al., (2021). Supraharmonics in Power Grid: Identification, Standards, and Measurement Techniques. *IEEE Access, Vol. 9, pp. 103677-103689*. <https://ieeexplore.ieee.org/document/9492140>
- Ali M. Eltamaly, et. al., "Mitigation Voltage Sag Using DVR with Power Distribution Networks for Enhancing the Power System Quality", *International Journal of Electrical Engineering and Applied Sciences (IJEEAS)*, Vol. 1, No. 2, October 2018.
- Alkahtani, Ammar A., et al., (2020). Power Quality in Microgrids Including Supraharmonics: Issues, Standards, and Mitigations. *IEEE Access, Vol.8, pp. 127104 - 127122*. <https://ieeexplore.ieee.org/document/9136692>
- Arsha, S., et. al., (2017). Comparison of Voltage Sag and Swell Mitigation Using DVR and D-STATCOM. *International Journal of Advance Research in Engineering, Science & Technology, Volume 4, Issue 4*.
- Bohan Liu, Xiang Ping Ni, Guzheng Yan, Bo Li and K. Jia, (2016). Performance of ROCOF Protection in PV System. *IEEE, PES Asia-Pacific Power and Energy Conference - Xi'an –China*.
- Bozalakov, D.V., et. al., (2019). Overvoltage and voltage unbalance mitigation in areas with high penetration of renewable energy resources by using the modified three phase damping control strategy. *Electric Power Systems Research 168*. <https://doi.org/10.1016/j.epsr.2018.12.001>
- Cheng, J. (2017). IEEE Standard 519-2014 Compliances, Updates, Solutions and Case Studies. *2017 IEEE Power & Energy Society General Meeting*. DOI: 10.1109/PESGM.2017.8273773
- European Power Quality Survey Report, (2018). *Leonardo Energy*. <https://www.slideshare.net/sustenergy/european-power-quality-survey-report>
- Guerrero-Rodríguez, N.F., et. al., (2017). Synchronization Algorithms for Grid-Connected Renewable Systems: Overview, Tests References 93 and Comparative Analysis. *Renewable and Sustainable Energy Reviews, Vol.75, pp.629-643*.
- Hafez, M., et. al., (2019). Voltage Sag Enhancement in Microgrid with Applications on Sensitive Loads. *JAUES, Vol. 14, No. 50, 121-128*.

- Hassan, A., et. al., (2014). Modeling and Simulation of Integrated SCV and AEF using MATLAB & ETAP. *16th International Middle- East Power Systems Conference -MEPCON'2014*
- Hossain, E., et. al., (2018). Analysis and Mitigation of Power Quality Issues in Distributed Generation Systems Using Custom Power Devices. *IEEE Access*, pp. 16816-16833, Vol. 6.
- IEEE Std 1250, (2018). IEEE Guide for Identifying and Improving Voltage Quality in Power Systems. *IEEE Power and Energy Society*.
- IEEE Std 1564, (2014). IEEE Guide for Voltage Sag Indices. *IEEE Power and Energy Society*.
- International Energy Agency, (2021). Renewables 2021 Analysis and forecast to 2026. Revised version. <https://www.iea.org/corrections>.
<http://www.oecd.org/about/publishing/corrigenda.htm>
- International Standard IEC 61000-4-19, Part 4-19, (2014). Testing and measurement techniques – Test for immunity to conducted, differential mode disturbances and signalling in the frequency range 2 kHz to 150 kHz at a.c. power ports. IEC 61000-4-19:2014 - Electromagnetic Compatibility (EMC) - Part 4-19: Testing and Measurement Techniques - Test for Immunity to Conducted, Differential Mode Disturbances and Signalling in the Frequency Range 2 kHz to 150 kHz at A.C. Power Ports | Interference Technology
- International Standard IEC 61000-4-3, Part 4-3, (2006). Testing and measurement techniques- Radiated, radio-frequency, electromagnetic field immunity test. IEC 61000-4-3 - Electromagnetic compatibility (EMC) – Part 4-3: Testing and measurement techniques – Radiated, radio-frequency electromagnetic field immunity test | Engineering360 (globalspec.com)
- International Standard IEC 61000-4-7, Part 4-7, (2002). Testing and measurement techniques – General guide on harmonics and interharmonics measurements and instrumentation, for power supply systems and equipment connected thereto. IEC 61000-4-7 pdf download - Electromagnetic compatibility (EMC) – Part 4-7: Testing and measurement techniques – General guide on harmonics and interharmonics measurements and instrumentation, for power supply systems and equipment connected thereto - IEC standards online
- Kumar, K. A., et. al., (2016). Recent Advances and Control Techniques in Grid Connected PV System – A Review. *International Journal of Renewable Energy Research*, Vol.6, No.3, pp.1037-1049.
- Kumar, S. A., Vanurrappa, D. (2011). Voltage Dip mitigation in Distribution System by Using DStatcom. *Journal of Energy Technologies and Policy*, Vol.1, No.1.
- Kumara, P. P., et. al., (2021). Performance Improvement Of Grid Tied PV System With VSC Based DVR For Voltage Sag. *Turkish Journal of Computer and Mathematics Education* Vol.12 No.12, 1772-1780.

- Li Ma, et. al., (2021). An Evaluation Method for Bus and Grid Structure Based on Voltage Sags/Swells Using Voltage Ellipse Parameters. *IEEE Access*, Vol. 9. DOI 10.1109/ACCESS.2021.3096329
- Longfu Luo, et. al., "Compensation Strategy for Multiple Series Centralized Voltage Sag in Medium Voltage Distribution Network", APPEEC2019.
- McGranaghan, M. (2006). Update on IEC 61000-3-6: Harmonic Emission Limits for Customers Connected to MV, HV, and EHV. *2005/2006 IEEE/PES Transmission and Distribution Conference and Exhibition*. <https://ieeexplore.ieee.org/document/1668668>
- Mustafa, A. M., et. al., (2021). System Level-Based Voltage-Sag Mitigation Using Distributed Energy Resources. *IEEE Systems Journal*, Vol. 15, No. 4.
- P. M. Arockia Dass, Omkar S Pawar, and A. Peer Fathima, "Voltage Sag and Harmonic Compensation of PV Fed Unified Power Quality Conditioner", *IJCTA*, 9(2) 2016, pp. 741-748, International Science Press.
- Prince Sinh and Chintan Patel, "The Role of DSTATCOM as Active Filter to Mitigate Harmonics in Distribution System", *IJSRD - International Journal for Scientific Research & Development* | Vol. 3, Issue 01, 2015.
- Shahgholian, G., (2021). A brief review on microgrids: Operation, applications, modeling, and control. *Int. Trans. Electrical Energy System*. <https://doi.org/10.1002/2050-7038.12885>
- Smriti, D. (2014). Comparison of DVR and D-STATCOM for Voltage Quality Improvement. *International Journal of Emerging Technology and Advanced Engineering*, Volume 4, Issue 10.
- Standard EN 50160, (2004). Voltage Disturbances: Voltage Characteristics in Public Distribution Systems. *Power Quality Blog*. Standard EN 50160 – Voltage Characteristics of Public Distribution Systems – Power Quality Blog
- Stevenson, W. J., (1955). Elements of power system analysis. *Book published by McGraw-Hill*.
- Sujata, M. B., et. al., (2020). Power Quality Improvement using a Shunt Active Power Filter for Grid Connected Photovoltaic Generation System. *978-1-7281-6828-9/20/\$31.00 ©2020 IEEE*.
- Taeyong Kang, et. al., "Series Voltage Regulator for a Distribution Transformer to Compensate Voltage Sag/Swell", *IEEE Transactions On Industrial Electronics*, Vol. 64, No. 6, June 2017.
- Tamas Kerekes, T., et. al., (2015). Three-phase Photovoltaic Systems: Structures, Topologies, and Control. *Electric Power Components and Systems*, Vol.43, No.12, pp.1364–1375.

- Tingting D., et. al., (2021). Circuit Principle and Design of Superconducting Shunt Resonator for Voltage Sag Mitigation. *IEEE Transactions on Applied Superconductivity*, Vol. 31, No. 8.
- Vishwakarma, J., Sharma, A. K. (2015). Simulation and Comparison of DVR and DSTATCOM Used for voltage sag mitigation at Distribution Side. *International Journal of Recent Research in Electrical and Electronics Engineering (IJRREEE)* Vol. 2, Issue 2, pp: (197-205).

APPENDIX A

Running a Load Flow Analysis by ETAP Program

The purpose of this Appendix is to introduce the Load Flow Analysis module and provide instructions on how to run a load flow study. In addition, an example of how to regulate bus voltage using transformer LTCs and how ETAP flags overload conditions will be given. Furthermore, there will be a brief look at the Load Flow Result Analyzer. For this tutorial you should select “Example Project (ANSI)” option when starting ETAP Demo.

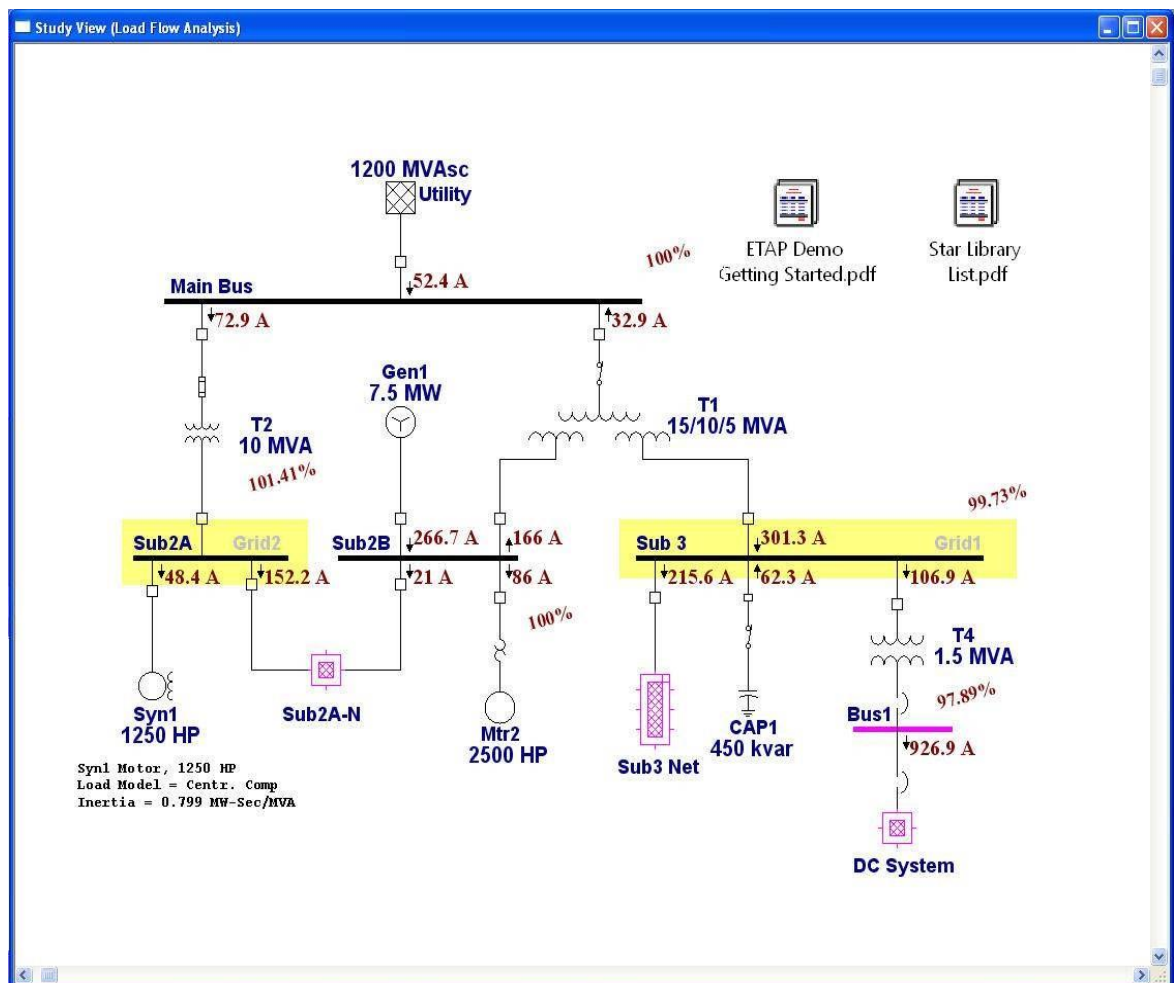


Figure A1. Example ANSI after running load flow analysis

A.1. Running Load Flow Analysis

Click the Load Flow Analysis button on the Mode toolbar to switch to Load Flow Analysis mode.



Figure A2. Toolbar showing the Load Flow Analysis button location

Running a Load Flow Analysis will generate an output report. In the Study Case toolbar, you can select the name of an existing output report to overwrite, or "Prompt." If "Prompt" is selected, then prior to running the Load Flow Analysis you will be prompted to enter a new report name.

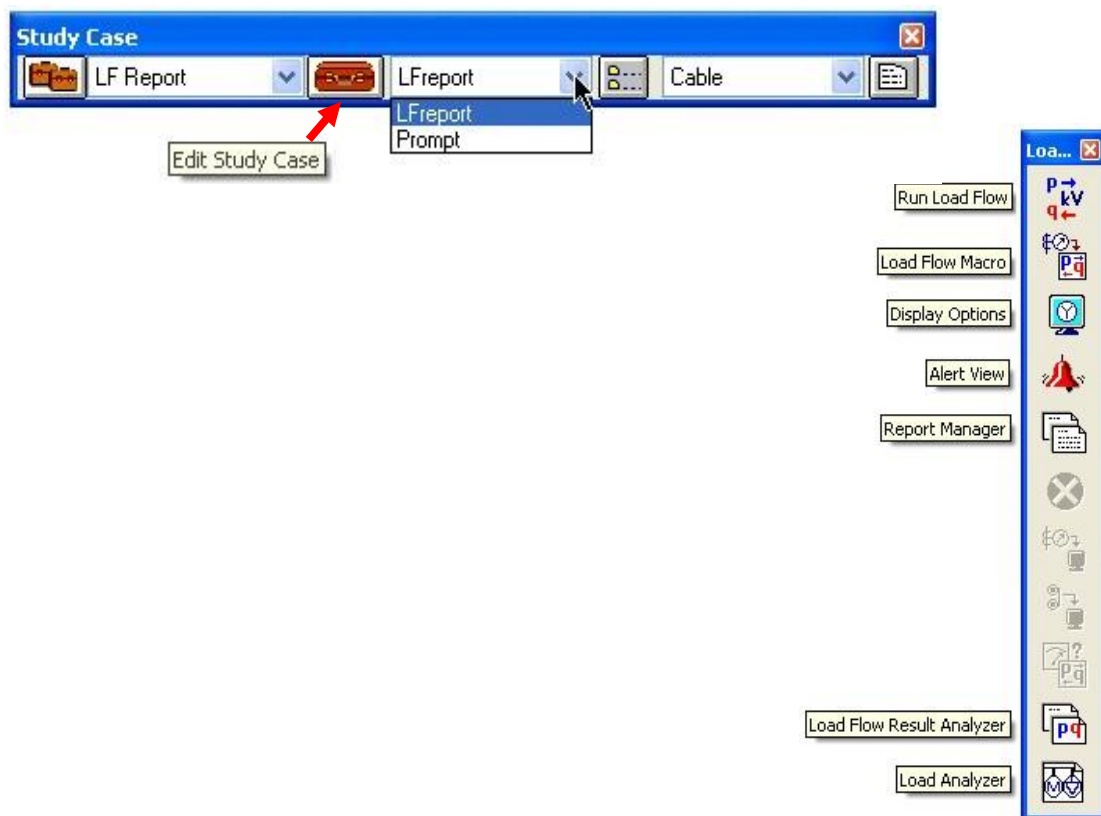


Figure A3. Locations of essential buttons for the analysis

One can customize your study by changing the options in the Load Flow Study Case editor. For example, different methods with maximum number of iterations and

precision can be specified; loading and generation categories can be individually selected; load diversity factors can be applied; and finally, adjustments can be selected for different elements, e.g., transformer, reactor, overload heater, cable, transmission line, and more.

A.2. Viewing the Results

To run the load flow study, click on the Run Load Flow button located in the Load Flow toolbar. After running the Load Flow Analysis, the results will be displayed on the one-line, as shown below:

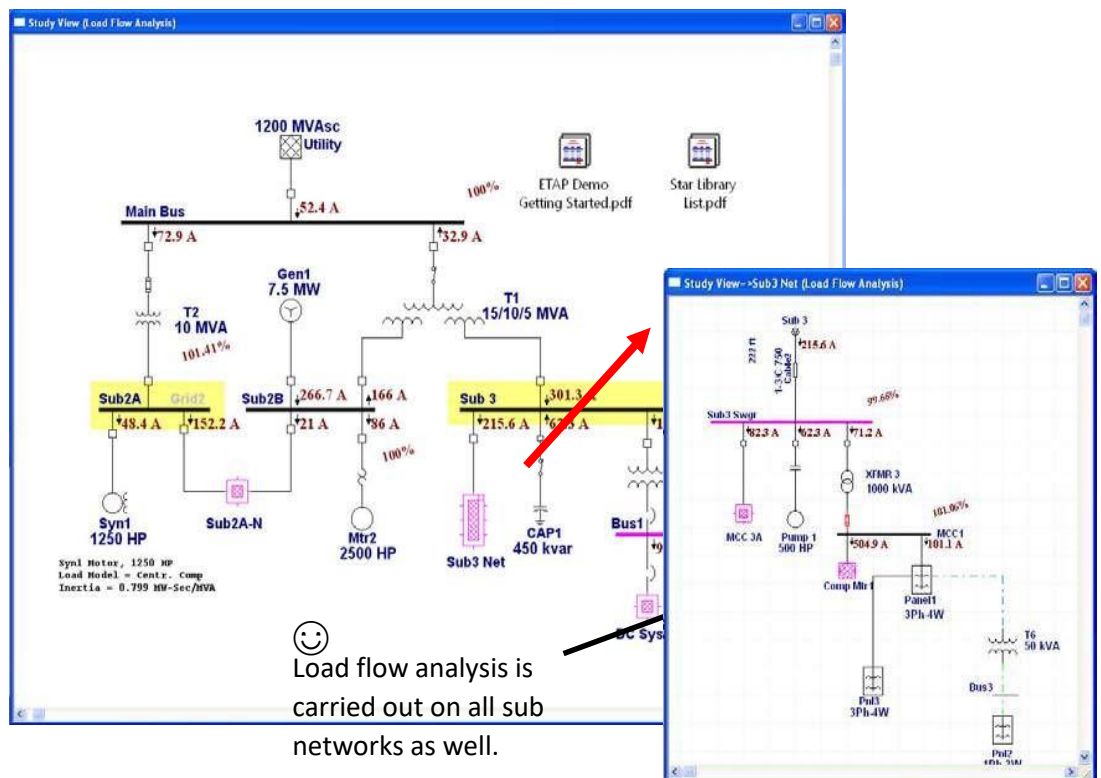
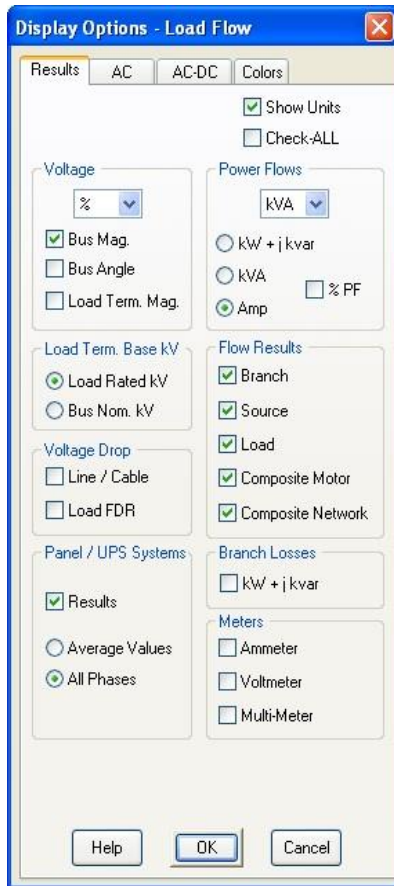


Figure A4. Helpful tips



The results shown on the one-line, and the format they are displayed in can be changed in the Display Options, which can be accessed from the Load Flow toolbar.

Figure A5. Options viewed to display required results

To view any overload problems, simply click the Alert View button in the Load Flow toolbar. This will open a window containing a list of undersized equipment. Please note that the alert view button is disabled in the ETAP Demo.

Critical						
Device...	Type	Rating	Calcula...	% Value	Condition	Phase ...
CB31	LV CB	800 Amp	926.392	115.8	OverLoad	3-Phase
CB32	LV CB	175 Amp	306.42	175.1	OverLoad	3-Phase
Fuse3	Fuse	390 Amp	1239.913	317.9	OverLoad	3-Phase
Gen1	Generator	0 Mvar	0		UnderEx...	3-Phase
XFMR 3	Transfor...	1 MVA	1.028	102.8	OverLoad	3-Phase
Marginal						
Device...	Type	Rating	Calcula...	% Value	Condition	Phase ...
Bus1	Bus	0.48 kV	0.47	97.9	UnderV...	3-Phase
Bus2	Bus	0.48 kV	0.465	96.8	UnderV...	3-Phase
Fuse2	Fuse	125 Amp	119.932	95.9	OverLoad	3-Phase
Sub3 Swgr	Bus	225 Amp	208.301	92.6	OverLoad	3-Phase

Figure A6. Alert View button in the Load Flow toolbar

Output reports provide a way to view a more detailed and organized representation of the results. Click on Report Manager in the Load Flow toolbar and go to the Result page and select Load Flow Report. As you can see, we offer different file formats for the output report.

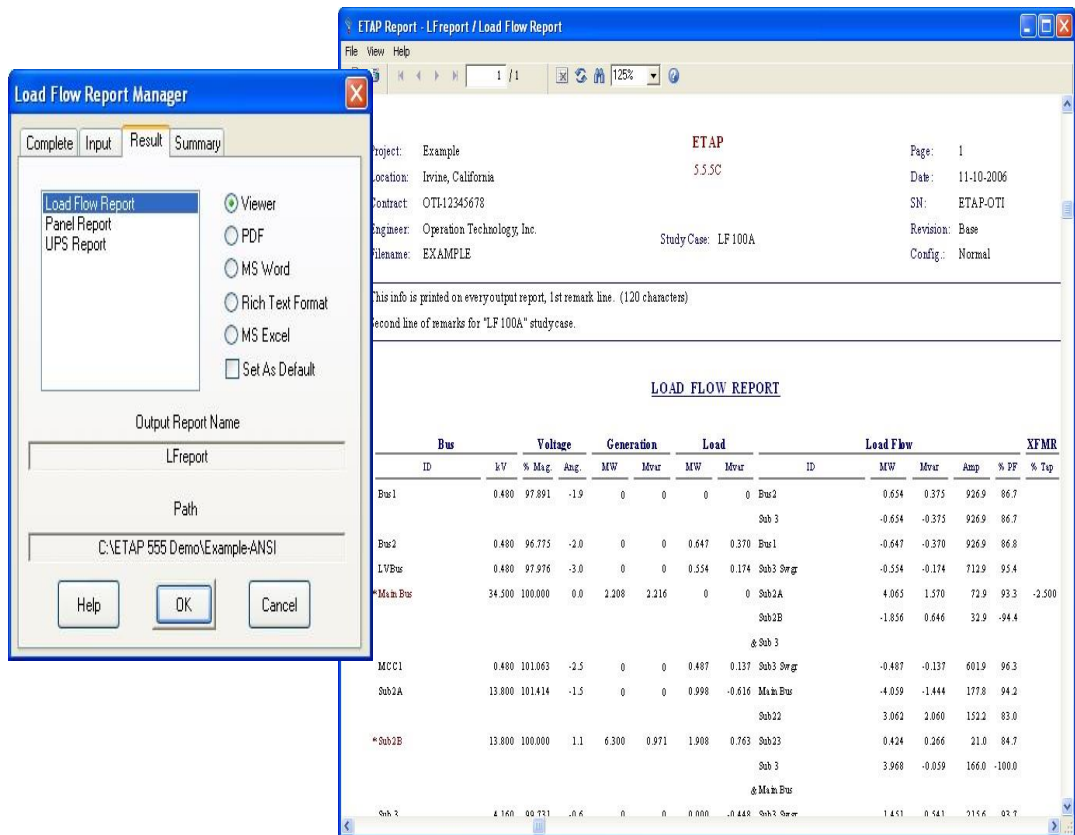
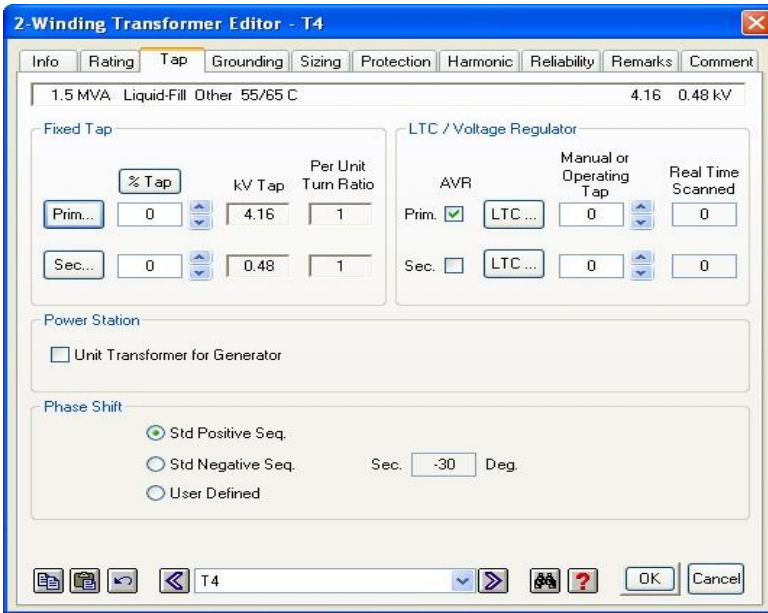


Figure A7. Setting the output report manager

A.3. Using the results

Looking at the results on the one-line, note that the operating voltage of Bus1 is 97.89%. This caused the bus to be flagged as marginally under voltage in the Alert View window. The criteria for which a condition is flagged can be changed in the Load Flow Study Case editor. We will now use the bus voltage regulation feature of the Transformer Editor to improve our Load Flow results.



ETAP allows Auto LTC settings to be applied to regulate buses that are directly or indirectly connected to a transformer. For example, we can use transformer T4 to regulate Bus1 at 100% of nominal voltage. Open the editor of T4 by double clicking on its graphic on the one-line. On the Tap page, enable (check) the Auto LTC box on the primary winding.

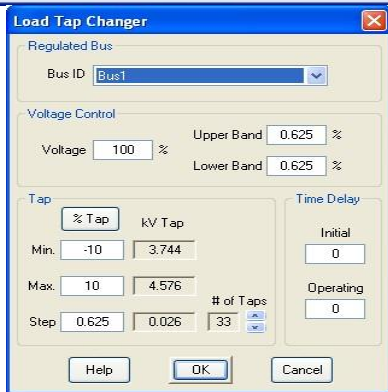


Figure A8. Setting the Load Tap Changer for the transformer

Open the LTC settings window by clicking on the LTC box and change the Regulated Bus ID to Bus1. Click OK for both the LTC window and the Transformer Editor window.

Run the Load Flow study again, with attention paid to the operating voltage of Bus1. Notice that the operating voltage of Bus1 is now within a tap step of the desired 100% regulation value. This is just one example of the many features of the ETAP Load Flow module.

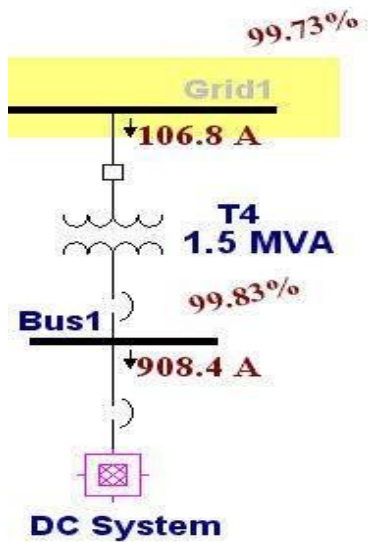


Figure A9. Results could be shown on SLD view

A.4. Analyzing the Results

The screenshot shows the 'Load Flow Result Analyzer' software interface. The main window displays a table of results with the following data:

ID	Rating	Rated kV	kvar	kW	Amp	% PF	% Loading	Vterminal
CAP1	-450 kvar	4.16	-448	0	62.29	0	93.7	99.73
Load1	280 kVA	0.48	121	238	328.9	89.16	97.5	97.52
LTG Load	100 kVA	0.48	0	102	121.6	100	100	101.06
LUMP1	220 kVA	0.46	110	194	273.7	87	98.1	102.24
LUMP2	3500 kVA	3.3	1889	3048	609	85	99.5	103.01
LUMP5	500 kVA	3.45	263	424	83.8	85	100.2	99.61
MOV1	14,743 HP	0.46	0	0	0	0		102.24
Mtr2	2500 HP	13.2	762	1902	85.97	92.83	95.9	104.26
Mtr3	75 HP	0.46	26.927	60.474	78.79	91.35	94.8	105.46
Mtr4	125 HP	0.46	44.397	101	131.1	91.51	94.8	105.46
Mtr5	50 HP	0.46	19.389	40.962	53.95	90.39	94.9	105.43
Mtr6	120 HP	0.46	44.979	97.606	127.9	90.82	100.0	105.46
Pump 1	500 HP	4	184	407	62.31	91.09	96.6	103.55
Syn1	1250 HP	13.2	-617	995	48.37	-85	94.5	105.63
Syn2	150 HP	0.46	-58.505	121	165.5	-90	98.2	101.8

The interface also includes several configuration panels: 'Study Reports' with a table for reports; 'Project Report' with 'Active Project' set to 'EXAMPLE'; 'Report Type' with 'Loads' selected; 'Load Type' with checkboxes for Induction, Synchronous, Lumped, Static, MOV, Capacitor, SVC, and Filter; 'Load Info' with checkboxes for Terminal Bus, Type, Rating, and Rated kV; 'Load Flow Results' with checkboxes for kW Loading, kvar Loading, Amp Loading, % PF, % Loading, and Terminal Voltage; and 'Alert' settings for Loading (100% Critical, 95% Marginal), OverVoltage (105%), and UnderVoltage (95%).

Figure A10. Load Flow Result Analyzer

After running the Load Flow study, you can analyze the output data for different elements in a very compact and summarized way by using the Load Flow Results Analyzer. To do so, click on the Load Flow Result Analyzer button in the Load Flow toolbar.

Select the different reports that you want to consider from the Study Reports field. If you want to compare output reports from other projects along with the current project, you can select All Project in Active Directory from the Project Report field. The other projects must be in the same directory as your current project.

Select the report type from the Report Type field. The example above shows results for Loads. After selecting Loads, select the Load Types and Load Info to display. Select the units to display the results in, and the different fields that you want to display. In addition, you can create your own alerts and enable them from the Alert field.

The commercial and nuclear versions of ETAP allow you to export the filtered results from the Load Flow Result Analyzer to an Excel spreadsheet.

